

CONFIDENTIAL  
Approved by OGC  
1/19/88

Los Alamos National Laboratory is operated by the University of California for the United States Department of Energy under contract W-7405-ENG-36

LA-UR--88-1753

DE88 014474

TITLE THE GNASH PREEQUILIBRIUM-STATISTICAL NUCLEAR MODEL CODE

AUTHOR(S) EDWARD D. ARTHUR

SUBMITTED TO PROCEEDINGS OF THE ICTP WORKSHOP ON APPLIED NUCLEAR THEORY AND NUCLEAR MODEL CALCULATIONS FOR NUCLEAR TECHNOLOGY APPLICATIONS  
(15 February - 18 March 1988)

**DISCLAIMER**

This report was prepared as an account of work sponsored by an agency of the United States Government. Neither the United States Government nor any agency thereof, nor any of their employees, makes any warranty, express or implied, or assumes any legal liability or responsibility for the accuracy, completeness, or usefulness of any information, apparatus, product, or process disclosed, or represents that its use would not infringe privately owned rights. Reference herein to any specific commercial product, process, or service by trade name, trademark, manufacturer, or otherwise does not necessarily constitute or imply its endorsement, recommendation, or favoring by the United States Government or any agency thereof. The views and opinions of authors expressed herein do not necessarily state or reflect those of the United States Government or any agency thereof.

By acceptance of this article the publisher recognizes that the U.S. Government retains a nonexclusive, royalty-free license to publish or reproduce the published form of this contribution or to allow others to do so for U.S. Government purposes.

The Los Alamos National Laboratory requests that the publisher identify this article as work performed under the auspices of the U.S. Department of Energy.



**Los Alamos** Los Alamos National Laboratory  
Los Alamos, New Mexico 87545

mla

# The GNASH Preequilibrium-Statistical Nuclear Model Code

E. D. Arthur

Theoretical Division

Los Alamos National Laboratory

Los Alamos, New Mexico USA

## Abstract

The following report is based on materials presented in a series of lectures at the International Center for Theoretical Physics, Trieste, which were designed to describe the GNASH preequilibrium statistical model code and its use. An overview is provided of the code with emphasis upon the code's calculational capabilities and the theoretical models that have been implemented in it. Two sample problems are discussed, the first dealing with neutron reactions on  $^{58}\text{Ni}$ . The second illustrates the fission model capabilities implemented in the code and involves  $n + ^{235}\text{U}$  reactions. Finally a description is provided of current theoretical model and code development underway. Examples of calculated results using these new capabilities are also given. This material is organized into three sections as follows:

Section I - GNASH code overview and theoretical models,

Section II - Code structure and problem input/output description,

Section III - New development efforts.

## SECTION I - OVERVIEW AND NUCLEAR MODELS

### I. Introduction

Three sections are used to describe the GNASH multistep Hauser Feshbach preequilibrium nuclear model code. They describe the model formalism(s), the capabilities of the code, and provide an overview of input required and output obtained. The content of these three sections are:

- 1.) GNASH overview and introduction to the theoretical models used and their implementation within the code;
  - 2.) Continuation of model description, code structure, and problem setup;
- and
- 3.) Current GNASH development.

### II. GNASH Overview

GNASH uses a multistep implementation of Hauser-Feshbach theory to calculate decay sequences from up to 10 compound nuclei in a given calculation for one or several incident particle energies. Preequilibrium corrections based upon the exciton model of Kalbach<sup>1</sup>, modified to include nuclear surface effects, are applied to the decay of the first compound nucleus. Up to 6 types of radiation can be emitted from each compound system so that in one calculation a maximum of 60 reaction paths can be treated. To facilitate such complicated reaction schemes, several options for automatic setup are available. Fig 1 provides an example of a reaction sequence included in a recent calculation of  $n + {}^{64}\text{Zn}$  reactions.

To perform such calculations GNASH uses information from several input files as illustrated in Fig 2. The primary data needed are (1) a mass and ground-state spin table, (2) a file containing transmission coefficients (penetrabilities obtained from spherical or deformed optical model calculations), and (3) discrete level data. For problems involving inelastic scattering from permanently deformed or vibrational nuclei, direct reaction contributions can be provided.

Output is also illustrated in the figure. The GNASH version to be described in these lectures provides angle-integrated cross sections and spectral data for both particle and gamma ray emission. Newer GNASH versions also provide angle-dependent spectra based upon use of new expressions developed by C. Kalbach<sup>2</sup> to describe the phenomenology of continuum particle emission angular distributions. A second method uses the free scattering kernel in the generalized exciton model to produce angular distributions.

Other GNASH features that are discussed are as follows. Two nuclear level density models - the Gilbert Cameron<sup>3</sup> and back-shifted Fermi gas<sup>4</sup> - are available and are adjusted to best fit discrete level data provided during the course of problem execution. A second feature concerns the choice of either the Weisskopf or Brink Axel form for gamma ray

transmission coefficients. In the latter case the detailed shape of the gamma ray strength function can be given as input to the calculation, thereby providing considerable flexibility in optimizing calculated gamma ray production spectra. Additionally the present code version includes a rather detailed fission model, where for each compound system, up to three uncoupled oscillators can be used to represent the fission barrier. At each barrier fission transition states can be generated automatically given bandhead information provided by the user. Fission barrier state densities are also modified (with an excitation-energy dependent factor) to account for differing nuclear shapes existing at each barrier.

As a final point of introduction it should be noted that GNASH was developed primarily for use at incident energies above those where width-fluctuation correction factors are important. The code does not calculate such corrections explicitly, but such information can be provided from external calculations. This allows GNASH to be used at lower energies with reasonable accuracy.

### III. Nuclear Models in GNASH

The Hauser Feshbach statistical model provides the basis for the majority of the cross section calculations performed in GNASH. The principal assumption used in the calculation of cross sections and emission spectra from complex reaction processes is that the reaction proceeds in a series of binary reaction stages. At each stage particle and gamma ray emission are calculated. This process is illustrated schematically in Fig 3. An initial compound nucleus is formed with excitation energy  $U$  and spin, parity  $J\Pi$ . This process (and all others occurring in the calculation) are subject to constraints imposed by the following conservation laws.

$$\begin{array}{lll}
 \epsilon + B_a = \epsilon' + E' + B_a & U & \text{energy} \\
 i + l + \underline{L} = i' + l' + \underline{L}' & J & \text{spin} \\
 p \otimes P \otimes (-1)^{\underline{L}} = p' \otimes P' \otimes (-1)^{\underline{L}'} & \Pi & \text{parity}
 \end{array} \quad (1)$$

where  $\epsilon, \epsilon'$  are center of mass energies of incoming and outgoing particles,  $B_a$  and  $B_a'$  are binding energies relative to the compound system,  $i, l, p, P$  are spins and parities associated with light particles and the heavier target or residual nucleus and  $\underline{L}$  is the orbital angular momentum. Primed quantities indicate the outgoing channel.

Each nucleus occurring in the calculation is assumed to be comprised of a series of discrete levels having specified values of  $E_i, J_i, \Pi_i$  above which a continuum of excitation energies occurs which is described using a level density model. Figure 4 illustrates this schematically. In GNASH integration over this continuum is accomplished by dividing it into equispaced regions of width  $\Delta E$ . This integration method is generally adequate for most problems, but an option is allowed for further splitting of the first 2-3 bins into finer integration

bins for increased accuracy, especially around reaction thresholds.

For most calculations the separation energy for particle emission occurs well into this continuum region. However for light nuclei known discrete level data may include levels that are unstable to particle emission. GNASH thus allows computation of particle decay from such levels.

The population of continuum bins  $P^{(n+1)}$  that occur in the  $(n+1)^{\text{th}}$  compound system formed by decay of the  $n^{\text{th}}$  compound system is calculated via use of the expression:

$$P^{(n+1)}(UJ\Pi) = \int dU' \sum_{J'\Pi'} P^n(U'J'\Pi') \frac{\Gamma^n(U'J'\Pi', UJ\Pi)}{\Gamma(U'J'\Pi')} \rho^{(n+1)}(UJ\Pi) \quad (2)$$

where  $P^{(n)}$  is the population of a given continuum bin specified by  $U'J'\Pi'$  in the  $n^{\text{th}}$  compound system,  $\Gamma^n$  is the partial width appropriate for a decay from a system specified by  $U'J'\Pi'$  to a continuum bin in the  $(n+1)^{\text{th}}$  compound system specified by  $UJ\Pi$ . This formalism also allows the explicit calculation of gamma-ray cascades if one considers that the  $n+1$  and  $n^{\text{th}}$  system are identical and are linked together computationally by gamma-ray emission. The calculational order used in GNASH (to be described later) handles gamma-ray emission from a given continuum bin first, so that the starting population for particle decay has been modified for gamma-ray population and depopulation. Figure 5 provides more schematic detail regarding the processes involved in the decay of a given compound system.

The initialization of this decay sequence begins via the calculation of the cross section for formation of the first compound nucleus. This cross section is determined by summing over transmission coefficients at the center of mass energy appropriate for the incident channel via

$$\sigma_a(EIP, UJ\Pi) = \frac{\pi}{k^2} \frac{(2J+1)}{(2I+1)(2i+1)} \sum_{S=|I-i|}^{I+i} \sum_{\ell=|J-S|}^{J+S} f_{\ell} T_{\ell}(E) \quad (3)$$

Thus  $P^{(1)}(UJ\Pi) = \sigma_a \delta(U - \epsilon - B_a)$ . The quantity  $\Gamma^n(U'J'\Pi', UJ\Pi)/\Gamma(U'J'\Pi')$  represents the branching ratio of a partial width for a given decay to the total width. The total width is the sum over all such decay channels. The ratio of the partial to total width is determined via

$$\frac{\Gamma(U'J'\Pi', UJ\Pi)}{\Gamma(U'J'\Pi')} = \frac{1}{N(U'J'\Pi')} \sum_{\ell, S} T_{\ell}(U' - U - B_n) \quad (4)$$

where  $B_n$  is the binding energy associated with the decay of interest (zero for gamma ray emission),  $U$  is the residual energy left by an emission of energy  $\epsilon$  during the decay. The Hauser Feshbach denominator is the sum over all open channels consistent with the

angular momentum and parity rules indicated in (1). It contains contributions from both continuum-continuum and continuum-level transitions:

$$N(U'J'\Pi') = \sum_{I,P} \int d\epsilon T(\epsilon) \rho(U'-\epsilon) + \sum_i T(U-U'-E_i) \quad (5)$$

Here and in expression (2)  $\rho$  is the density of nuclear levels at a given excitation energy  $U'-\epsilon$  in the residual nucleus while the  $T$ 's are transmission coefficients evaluated using optical model penetrability data or an appropriate model for gamma rays.

#### IV: Evaluation of the Components of the Hauser Feshbach Expressions

##### A. Level Density Models - Gilbert Cameron

The level density model implemented in GNASH which has been used in most calculations is that of Gilbert-Cameron. This model uses a Fermi gas form at higher excitation energies along with a constant temperature form for lower energies. These two components were illustrated in Fig3. The level density form is given by

$$\rho(EJ\Pi) = \frac{(2J+1) \exp[-(J+1/2)^2 / 2\sigma^2]}{2\sqrt{2\pi} \sigma^2} \rho(U) \quad (6)$$

where  $U = E - \Delta$  ( $\Delta$  is the pairing energy) and  $\sigma^2$  is the spin cutoff parameter determined via

$$\sigma^2 = C \sqrt{aU} A^{2/3} \quad (6a)$$

where  $a$  is the Fermi gas parameter. Two options are available in GNASH for evaluation of  $\sigma^2$ . The first (and default) uses  $C=0.146$  as determined by Reffo while the second uses the original Gilbert Cameron value of 0.088. To evaluate  $\rho(E)$  in this model either a Fermi gas form is used (above  $E_x > E_{\text{match}}$ )

$$\rho(U) = \frac{\sqrt{\pi}}{12} \frac{1}{2\sqrt{\pi} \sigma} \frac{\exp(2\sqrt{aU})}{a^{1/4} U^{5/4}} \quad (7a)$$

or a constant temperature ( $E_x < E_{\text{match}}$ )

$$\rho(E) = \frac{1}{T} \exp \frac{(E - E_0)}{T} \quad (7b)$$

The pairing energy used to determine U in (7a) is determined from the Cook parameter set<sup>5</sup> for P(Z) and P(N). The Fermi gas parameter a is determined (in the default mode) via

$$a/A = 0.00917 [ S(Z) + S(N) ] + C \quad (7c)$$

where the shell factors S(Z) and S(N) again are those based on the Cook parameter set and C= 0.120 for a deformed nucleus and 0.142 for spherical cases. In the determination of level densities in the code, the assumption is made that there is an equal probability for positive or negative parity. Thus a factor of 1/2 multiplies Eq (6).

GNASH automatically adjusts  $E_0$ , T, and  $E_{\text{match}}$  by requiring that

$$\begin{aligned} \rho_T(E_m) &= \rho_{FG}(E_m) \\ \rho'_T(E_m) &= \rho'_{FG}(E_m) \end{aligned} \quad (8)$$

$$\int_0^{E_c} \rho_T(E) dE = N_{\text{exp}}(E_c)$$

Here  $N_{\text{exp}}$  is the cumulative number of levels that exist up to an excitation energy  $E_c$ . This information can be provided by the user via the problem input or it can be taken automatically from the level data file used during problem execution.

## B. Level Density Models - Back Shifted Fermi Gas

A second option for level density calculations in GNASH involves use of the back-shifted Fermi-gas model as implemented by Dilg<sup>4</sup>. Here one form of the level density describes the entire excitation energy region.

$$\rho(U) = \frac{1}{12\sqrt{2}} \frac{1}{\sigma a^{1/4}} \frac{\exp(\sqrt{2au})}{(U+t)^{5/4}} \quad (9)$$

where the spin cutoff parameter is evaluated via

$$\sigma^2 = 0.015 t A^{5/3} \quad (9a)$$

and the nuclear temperature  $t$  is defined by

$$U = at^2 - t \quad (9b)$$

The spin dependent level density is then determined using eq.(6).

### C. Transmission Coefficients

Particle emission transmission coefficients are determined from optical model calculations as mentioned earlier. Gamma ray transmission coefficients are calculated using either the Weisskopf single particle model<sup>6</sup> or the Brink-Axel<sup>7</sup> giant dipole resonance model. For the Weisskopf model the gamma ray transmission coefficient is computed as

$$T_W^l(\epsilon_\gamma) = K_W \epsilon_\gamma^{(2l+1)} \quad (10a)$$

For the Brink Axel model a giant dipole resonance form is assumed for E1 and M1 radiation so that

$$T_{BA}^{E1,M1}(\epsilon_\gamma) = K_{BA} (0.013 A) \frac{2}{\pi \hbar^2 c^2} \frac{\epsilon_\gamma \Gamma}{(E^2 - \epsilon_\gamma^2) + (\epsilon_\gamma \Gamma)^2} \quad (10b)$$

In this expression  $E$  and  $\Gamma$  are provided as input for E1 radiation while for M1 radiation default values of  $E = 8$  MeV and  $\Gamma = 5$  MeV are assumed.

The constants can be determined through fitting neutron s-wave resonance data  $2\pi\langle\Gamma_\gamma\rangle/\langle D\rangle$  data or through determination of a gamma ray strength function. For direct utilization of neutron resonance data GNASH determines the gamma ray transmission coefficient normalization from

$$\frac{\langle\Gamma\rangle}{\langle D_0\rangle} = \frac{1}{2\pi} \int_0^{B_n} \sum_{J\Pi} T_\gamma(\epsilon_\gamma = B_n - U) \rho(U, J\Pi) d\epsilon_\gamma \quad (11)$$

Alternatively the gamma ray transmission coefficient normalization can be obtained through determination of the gamma ray strength function by fitting neutron capture data in the mass



region of interest for a given set of calculations. The strength function is defined (for the Brink Axel giant dipole resonance model) as

$$f_{BA} = \frac{k \epsilon_{\gamma} \Gamma}{(\epsilon_{\gamma}^2 \Gamma^2) + (\epsilon_{\gamma}^2 - E_R^2)^2} \quad (12a)$$

which is related to the gamma ray transmission coefficient by

$$T_{\gamma}^{\ell} = f_{\gamma}^{\ell} \epsilon_{\gamma}^{(2\ell+1)} \quad (12b)$$

Utilization of the gamma ray strength function normalization directly avoids, in many problems, difficulties arising from extrapolation of s-wave resonance data to unmeasured cases as well as problems arising from level density contributions that arise in the evaluation of Eq (11).

## V. Additional GNASH Models

### A. Preequilibrium Model

After calculation of populations of the first compound nucleus using the Hauser Feshbach expressions discussed here, corrections for nonequilibrium reaction mechanisms (preequilibrium and direct-reaction effects) can be made on populations and particle emission spectra. The major part of these contributions are calculated using the exciton preequilibrium model as formulated by Kalbach in her code PRECO-B<sup>8</sup>. The corrections are applied after the initial Hauser Feshbach calculations have been made. The reasons for doing this will be addressed later in the discussion of the renormalization of spectra and population increments.

The exciton model involves solution of a series of master equations that describe the equilibration of an excited system through a series of binary collisions leading to more complex configurations of particle-hole pairs. Specifically

$$\frac{dP(n,t)}{dt} = \lambda^{+}(n-2)P(n-2,t) + \lambda^{-}(n+2)P(n+2,t) - [\lambda^{+}(n) + \lambda^{-}(n) + W(n)]P(n,t) \quad (13)$$

where  $P(n,t)$  is the probability that the excited nuclear system exists in the exciton state  $n$  ( $n=p+h$ ) at time  $t$ ;  $\lambda^{+}$  and  $\lambda^{-}$  are internal transition rates for  $n \rightarrow n+2$  and  $n \rightarrow n-2$  respectively; and  $W(n)$  is the total particle emission rate from a given exciton configuration summed over

all outgoing particles and energies. The initial condition for solution of these equations is

$$P(p,h,0) = \delta_{p,p_0} \delta_{h,h_0}$$

Angle integrated cross sections are calculated via

$$\frac{d\sigma}{d\varepsilon}(a,b) = \sigma_a \sum_n w_b(n,\varepsilon) \tau(n) \quad (14)$$

where  $\tau(n)$  is the mean lifetime for the exciton state defined by

$$\tau(n) = \int_0^T P(n,t) dt \quad (15)$$

and  $w_b(n,\varepsilon)$  is the average rate for emission of particle b with energy  $\varepsilon$  from the  $n^{\text{th}}$  exciton state.

To solve eq(13) the following quantities must be calculated. The state density for a given p-h configuration existing at an excitation energy E is given

$$\omega(p,h,E) = \frac{g_0^n (E - A_{p,h})^{p+h-1}}{p! h! (p+h-1)!} \quad (16)$$

where  $A_{ph} = E_{\text{Pauli}}(p,h) - (p^2 + h^2 + n)/4g_0$  and  $E_{\text{Pauli}} = \max(p,h)/g_0$  is the minimum energy required for the configuration by the Pauli exclusion principle. The state density factor  $g_0$  is usually calculated as  $A/13$  or by relating it to the Fermi gas a parameter through  $g = 6a/\pi^2$ . Rates for transitions allowed by the assumption of binary collisions ( $\Delta n = \pm 2$ ) are

$$\begin{aligned} \lambda^+(p,h,E) &= \frac{2\pi}{\hbar} M^2 \frac{g_0^3 [E - E_{\text{Pauli}}(p+1,h+1)]^2}{2(n+1)} \\ \lambda^-(p,h,E) &= \frac{2\pi}{\hbar} M^2 \frac{g_0 p h (n-2)}{2} \\ &\otimes \left[ 1 - \frac{(n-1)(p-1)(p-2) + (h-1)(h-2)}{8 g_0 [E - E_{\text{Pauli}}(p,h)]} \right] \end{aligned} \quad (17)$$

where  $M^2$  is the matrix element for two-body interaction between a specific initial and final state and  $E_{\text{Pauli}}$  is the Pauli energy for the indicated configuration. In GNASH  $M^2$  is parameterized as a function of  $e = E/n$  via

$$\begin{aligned}
M^2 &= \frac{k}{Ae} \sqrt{\frac{e}{7 \text{ MeV}}} \sqrt{\frac{e}{2 \text{ MeV}}} & e < 2 \text{ MeV} \\
&= \frac{k}{Ae} \sqrt{\frac{e}{7 \text{ MeV}}} & 2 < e < 7 \text{ MeV} \quad (18) \\
&= \frac{k}{Ae} & 7 < e < 15 \text{ MeV} \\
&= \frac{k}{Ae} \sqrt{\frac{15 \text{ MeV}}{e}} & e > 15
\end{aligned}$$

The constant k is usually set to equal 130-160 MeV<sup>3</sup>.

In GNASH the state density for the initial p-h configuration is corrected to account for variations of the single-particle state density with energy in the potential well and to account for effects due to the finite depth of the nuclear potential. The first correction involves replacing  $g_0$  with

$$g(p_0, h_0, E) = \frac{g_0}{n_0} \left[ p_0 \sqrt{1 + \frac{E}{n_0 V}} + h_0 \sqrt{1 - \frac{E}{n_0 V}} \right] \quad (19)$$

To account for the effect of the finite depth of the nuclear potential in limiting the energy of hole degrees of freedom, the state density is modified via

$$\omega(p_0, h_0, E, V) = \omega(p_0, h_0, E, \infty) \left[ 1 - h_0 \left( \frac{E-V}{E} \right)^{n-1} \right] \quad (20)$$

for  $E > V$ . For most configurations  $V = 38$  MeV. However for the initial exciton configuration ( $n=3$ )  $V$  varies between 38 MeV for low incident energies down to 11 MeV at higher incident energies as determined from the following expression.

$$V = 11 + 27 \left[ 1 - \exp\left(-\frac{E-27}{5}\right) \right]^{-1} \text{ (MeV)} \quad (21)$$

This expression results from a phenomenology developed by Kalbach<sup>9</sup> to account for nuclear surface effects that occur at higher incident energies. It improves the agreement with higher emission energy portions of spectra produced at incident energies greater than 50 MeV.

The emission rate for particles of type b and emission energy  $\epsilon$  is

$$w_b(n, \epsilon) = \frac{(2s_b + 1)}{\pi^2 \hbar^3} \mu_b \sigma_b(\epsilon) \epsilon \, d\epsilon \frac{\omega(p - p_b, h, U)}{\omega(p, h, E)} Q_b(p) \quad (22)$$

where  $s_b, \mu_b, p_b$  are the spin, reduced mass, and nucleon number of the emitted particle, U is

the residual nucleus excitation energy,  $\sigma_b(\epsilon)$  is the inverse cross section evaluated at the emission energy of b, and  $Q_b$  is a factor that takes into account the distinguishability of neutrons from protons for a given particle configuration. Two methods are employed in GNASH to calculate  $Q_b$ . The first is based upon the assumption that in each pair-creation interaction, protons and neutrons are created with the relative probabilities  $Z/A$  and  $N/A$ . The second form assumes the neutron and proton p-h pairs are excited in proportion to the state densities of the configurations formed. More detail is provided in Los Alamos report LA-10248 10.

## B. Models for Other Nonequilibrium Processes

In addition to the preequilibrium cross sections and spectral contributions calculated using the exciton model, two other classes of nonequilibrium contributions can be included in GNASH calculations. The first accounts for direct-reaction contributions to inelastic scattering. These are determined via coupled-channel calculations using a code such as ECIS or through distorted wave Born approximation calculations performed with a code such as DWUCK.

A second, more general class of nonequilibrium contributions, are included automatically in GNASH nonequilibrium calculations. These are contributions arising from particle pickup, knockout, stripping, etc which are calculated using a phenomenology developed by Kalbach<sup>2</sup> which are discussed below. In particular these expressions are used to calculate composite-particle emission rather than through use of exciton model expressions modified to include "fit parameters" such as preformation constants.

To determine contributions due to pickup/stripping processes the semiempirical expression

$$\frac{d\sigma^{p-s}}{d\epsilon}(a,b) = (2s_b + 1) p_b \epsilon \sigma(\epsilon) \omega_F(U) (20)^{\delta_\alpha} \quad (23)$$

$$\otimes f\left(\frac{E_a}{p_a}\right)^{-2\Delta} \left(\frac{780}{A}\right)^\Delta 1.4 \times 10^{-4} (\text{MeV})^{2\Delta-1}$$

is used. Here  $\Delta$  is the number of transferred particles and  $\delta_\alpha = 1$  if an alpha is formed, -1 if one is destroyed, and zero otherwise. The function  $f$  is

$$f(N, Z, \Delta_\nu, \Delta_\pi) = (2Z/A)^{6\Delta_\pi} (2N/A)^{(1-\Delta_\pi)\Delta_\nu (\Delta_\nu + 1)/2} \quad (24)$$

where  $\Delta_\pi$  and  $\Delta_\nu$  are the number of transferred protons and neutrons respectively. The density of states is determined from

$$\omega_F^{p-s}(U) = \frac{\Delta I}{\Lambda_\pi! \Delta_\nu!} \sum_{i=1}^A \omega(0,i,U) \quad (25)$$

A second contribution describing knockout and inelastic processes involving alpha clusters is calculated from

$$\frac{d\sigma^{K-I}}{d\epsilon}(a,b) = \frac{\sigma_a}{p_a \epsilon_a^3} (2s_b + 1) p_b \epsilon \sigma_b(\epsilon) \quad (26)$$

$$\otimes \frac{\omega_F^{K-I}(U)}{A^2} F_a 0.12 \text{ MeV}^2 / \text{mb}$$

where  $F_\alpha = 1$ ,  $F_n = F_p = \frac{1}{2} Z/2A$ . The density function  $\omega_F^{KI}$  has the following forms depending upon the process involved.

(a.)  $\omega_1(U) = g_i g_\alpha (U - 1/2g_i - 2/g_\alpha)$   $i=n$  or  $p$ ;  $p,\alpha$  or  $n,\alpha$  knockout or  $(\alpha,p)$  or  $(\alpha,n)$  knockout

(b.)  $\omega_2(U) = g_\alpha^2 U$  elastic scattering with excitation of an alpha p-h pair

(c.)  $\omega_3(U) = g_n^2(U) + g_p^2(U)$   $(\alpha,\alpha')$  inelastic scattering exciting a nucleon pair.

In these expressions  $g_p = Z/(13 \text{ MeV})$ ,  $g_n = N/(13 \text{ MeV})$  and  $g_\alpha = A/(52 \text{ MeV})$ .

Once preequilibrium and other nonequilibrium contributions are computed, they are used to renormalize spectra and populations  $P(UJ\Pi)$ . For spectra this renormalization is accomplished by readjustment downward of the calculated compound nucleus contribution which is then added to that determined from the nonequilibrium models described above -

$$\frac{d\sigma}{d\epsilon} = F \left( \frac{d\sigma}{d\epsilon} \right)_{\text{CN}} + \left[ \left( \frac{d\sigma}{d\epsilon} \right)_{\text{non}} = \left( \frac{d\sigma}{d\epsilon} \right)_{\text{pre}} + \left( \frac{d\sigma}{d\epsilon} \right)_{\text{K-I}}^{p-s} \right] \quad (27)$$

The remaining compound nucleus fraction  $F$  is determined as

$$F = 1 - \frac{1}{\sigma_{\text{CN}}} \sum_b \left[ \int \left( \frac{d\sigma}{d\epsilon} \right)_{\text{pre}}^b d\epsilon \right] \quad (28)$$

If the compound nucleus cross section for a given energy bin is zero (corresponding to cases where widely-spaced discrete levels occur in the residual nucleus) then the calculated preequilibrium  $\sigma$  is also set to zero. To modify spin-dependent populations computed from continuum-continuum decay of the first compound nucleus, the assumption is made that the preequilibrium contribution (which is spin independent in this model) has the same distribution as the Hauser Feshbach results. Therefore

$$P(UJ\Pi) \text{ or } \left( \frac{d\sigma}{d\epsilon} \right)_{\text{K}} \text{ or } \left( \frac{d\sigma}{d\epsilon} \right)_{\text{CN}} = P_{\text{CN}}(UJ\Pi) \left[ F + \left( \frac{d\sigma(U)}{d\epsilon} \right)_{\text{noneq}} / \left( \frac{d\sigma(U)}{d\epsilon} \right)_{\text{CN}} \right] \quad (29)$$

Direct reaction effects are not included in this renormalization because in this case the  $\sigma_{CN}$  used in the preequilibrium and other expressions discussed above is renormalized downward by  $\sigma_{CN} = \sigma_{non} - \Sigma\sigma_{DI}$  to account for flux associated with direct reactions that is not appropriate for use in the calculation of Hauser Feshbach or preequilibrium emission.

### C. Fission

Within the Hauser Feshbach portion of GNASH fission can be included as a "decay" path . Up to three uncoupled barriers can be used to represent the fissioning system and each barrier has the characteristics illustrated in Fig 6. At each barrier transition states occur that are characterized by an energy above the barrier and spin,parity  $J\Pi$ . Analogous to the situation discussed earlier, discrete transition states are replaced by at higher energies above the barrier by a continuum which is described by the Gilbert Cameron level density model. Fission penetrabilities are determined by use of the Hill Wheeler expression for penetration through a parabolic barrier of height  $E_b$  and curvature  $\hbar\omega$

$$P_f = [1 + \exp(2\pi / \hbar\omega (E_b - E))]^{-1} \quad (30)$$

Since both discrete transition states and a continuum of such states occur, the total fission transmission coefficient is made up of two contributions, the first describing discrete transition states

$$T_F^{TS} = \sum_{TS} \frac{1}{(1 + 2\pi/\hbar\omega (E^{TS} - U))} \quad (31a)$$

and the second , the continuum of such states:

$$T_F^C(UJ\Pi) = \int_{E_L = -N\hbar\omega}^{E_c} d\varepsilon \rho(U - E_b + E_c - \varepsilon) P_f(\varepsilon) \quad (31b)$$

The fission model implemented in GNASH assumes the fully-damped limit so that the total fission width is determined via

$$T_F^{total}(UJ\Pi) = \frac{T_F^A \otimes (T_F^B + T_F^C)}{T_F^A + T_F^B + T_F^C} \quad (32)$$

In this limit no account is made of complications due to states existing in other wells. Width

fluctuation correction factors (when used) are set to one.

The specification of the transition state spectrum at each barrier can be made in two fashions. First the actual states can be provided directly ( $E_{XJ\Pi}$ ) by the user in which case the same spectrum of discrete states is assumed to exist at each barrier. Alternatively different sets of bandhead parameters can be provided for each barrier and the transition state spectrum is then automatically constructed by

$$E^{TS} = E_{\text{Band}} + \frac{\hbar^2}{2I} [J(J+1) - K(K+1)] \quad (33)$$

At higher energies above the barrier where a continuum of transition states occurs, the Gilbert Cameron level density model is used to calculate  $\rho^{TS}(U)$ . Provision is made for matching of the Fermi gas and constant temperature portions of this model using information provided or generated for discrete fission transition states. Finally the fission transition state density is modified through externally- provided factors which account for symmetry conditions existing at each barrier. Enhancements to the state density arise from the breaking of nuclear symmetries. Such enhancements can be related to the spin cutoff parameter  $\sigma$  and thus its dependence upon the energy above the barrier has been implemented in GNASH as varying as  $E^{1/4}$ . Additionally this enhancement is assumed to saturate at energies greater than about 15 MeV above the barrier as indicated (roughly) by the microscopic calculations of Jensen<sup>11</sup>. Thus the transition state density is modified from the value calculated with the Gilbert Cameron expressions by

$$\rho^{TS}(U) = f_0 (1 + U^{1/4}) \rho^{GC}(U) \quad (34)$$

Here  $f_0$  is the enhancement factor that is provided as input by the user.

Finally when fission calculations are made in combination with preequilibrium corrections the reaction cross section  $\sigma_a'$  available for use in the exciton model is reduced by the calculated fission cross section  $\sigma_a' = \sigma_a - \sigma_{\text{fiss}}$ . This procedure is based upon the assumption that fission occurs principally when the system has equilibrated and does not contribute during the early p-h reaction phases associated with preequilibrium processes.

## SECTION II- CODE STRUCTURE AND PROBLEM SETUP

### I. GNASH Code Structure

The structure of GNASH is illustrated in Fig 7. The main program module reads in problem-specific information from a card-image file. It also determines masses and binding energies as well as ground-state spins and parities through calls to the function ENERGY. A call to LEVPREP reads in discrete level information from TAPE8 while a call to TCPREP reads particle transmission data from TAPE10. A call to SETUP initializes level density, direct reaction, width fluctuation and spline parameters. This completes the portion of problem setup that is independent of incident energy. Then for each incident laboratory energy the following sequence occurs. SETUP2 is called to determine energies and integration end points as well as transmission coefficients for the incident channel. Direct reaction cross sections are also evaluated at the specified incident energy. The SPECTRA routine is called where the major portion of the cross section calculation process takes place. If preequilibrium corrections are desired then PRECMP is also called after calculations for the first compound nucleus have been completed. For most cases involving complicated reaction processes, the program continues within SPECTRA until the decay of all compound systems occurring in the problem has been determined. Finally DATAOUT is called to print output results and the process is repeated for the next incident energy. Listed below are the subroutines comprising GNASH.

- 1.LCSPACE - Sets up storage, determines parent reactions for specified decay sequences.
- 2.CHAINS- Constructs optional automatic reaction sequences.
- 3.ENERGY - Reads mass and ground state spin, parity from TAPE13
- 4.LEVPREP - Reads in level data from INPUT or more commonly from TAPE8. Prepares level data as needed for calculation. Calls SORT.
- 5.TCPREP - Reads in particle transmission coefficient from input or more commonly from TAPE10. Eliminates j-dependence of spin 1/2 arrays.
- 6.SETUP- Determines accumulated separation energies for decaying nuclei; identifies secondary reaction particles and photons, initializes level density parameters, reads direct reaction cross sections (if desired) from TAPE33 as well as width fluctuation factors.
- 7.SETUP2 - Determines energies appropriate to problem execution and integration end points. Generates transmission coefficients for the incident channel at a given center of mass energy and determines direct reaction cross sections appropriate for that energy.
- 8.SPECTRA- Main cross section calculation routine which is described in detail later. Calls LCMLOAD, GAMSET, INTERPI, PRECMP, and GRLINES. If fission is included calls RHOFIS, BAND, and TFIS.
9. INTERPI - Finds indices for interpolation.
- 10.Funct TFIS - Computes Hill-Wheeler penetrability



- 11.Funct RFIS - Computes fission transition state densities.
- 12.LEVDSET - Determines pairing and Fermi gas parameters. Calls GILCAM for Gilbert Cameron constant temperature and matching parameters and DOGET to compute  $D_{\text{observed}}$ .
- 13.GILCAM - Optimizes constant temperature expression parameters
- 14.LCMLOAD - Computes and stores transmission coefficients on energy grid required for  $i^{\text{th}}$  compound nucleus. Similarly calculates level density and yrast values. Provides a print of these quantities on integration grid if desired.
- 15.GAMSET - Sets up gamma ray cascade calculation. Determines Weisskopf or Brink-Axel parameters and gamma ray transmission coefficients on integration grid. Provides printout if desired. Calls FXCAL.
- 16.FXCAL - Computes gamma ray strength function.
- 17.WEISSKOPF - Computes normalization factor for gamma ray transmission coefficients. Calls FXCAL
- 18.INCHSUM - Performs sum over  $s$  and  $l$  of incident channel for a given compound nucleus spin and parity
- 19.GRLINES - Calculates discrete gamma ray cross sections, sums spectra to produce integrated cross sections, computes particle emission from particle unstable levels. Reads level data from TAPE9, calls ISERCH.
- 20.DATAOUT - Main output routine, calls LINEW2
- 21.LINEW2 - Utility for BCD single line writes, calls CXFP
- 22.CXFP - Allows more efficient E formatted writes.
- 23.PRECOMP - Main calling routine for preequilibrium corrections. Calls PRECOC. Renormalizes spectra, cross sections, and populations.
- 24.PRECOC - Based on PRECO-B program of Kalbach. Calls COMDEN, TTRANS, EMISS, RESOL, PICNOC, PRESPEC.
- 25.COMDEN - Determines composite nucleus state densities using Williams expressions. Calls WELL, OMEGA
- 26.TTRANS - Computes  $\lambda_+$ ,  $\lambda_-$ .
- 27.Funct QBETA - Determines  $Q_\beta$  for proton -neutron distinguishability
- 28.Funct OMEGA -Calculates  $(p,h)$  state densities.
- 29.PRESPEC - Determines preequilibrium emission spectra;prints results.
- 30.RESOL - Solves master equation as well as determines closed-form preequilibrium results.
- 31.EMISS - Calculates particle emission rates for a given p-h configuration. Determines total emission rate. Calls WELL, OMEGA, QBETA
- 32.PICNOC - Determines contributions due to pickup, knockout, and alpha particle reaction processes. Calls FACTOR, FF, OMEGA2.
- 33.Funct FACTOR - Computes factorial.
- 34.Funct FF - Computes  $f$  function needed for pickup, knockout.
- 35.Funct OMEGA2 - Computes state densities required for pickup, knockout, etc.
- 36.INTERP - Interpolation function

- 37.SPLINE - Spline function
- 38.Funct FUNDAC - Used in spline
- 39.AGET - Calculates Gilbert Cameron Fermi gas parameters for  $D_0$ .
- 40.DOGET - Calculates  $D_0$  from Gilbert Cameron a parameter.
- 41.WELL - Calculates finite well depth correction factors for use in determining surface effects in preequilibrium model
- 42.SORT - Sorts ZA data into ascending order.

## II. The SPECTRA Subroutine

The SPECTRA subroutine is the main calculational portion of the program, and in there partial and total widths, population increments as well as discrete level populations are computed for all compound systems occurring in a specified decay chain. Fig. 5 illustrates schematically the technique used to accumulate populations during these decay processes, while Fig. 8 provides a more complete description of the method used to compute binary reaction processes involved in particle or gamma ray decay.

Several nested DO loops are used to handle the entire reaction sequence. As illustrated in Figure 8 the outermost loop sums over all compound nuclei appropriate for the problem. The next loop sums over all energy bins (specified by K) in the decaying compound nucleus defined by the first loop. Once a continuum bin is identified, a third loop sums over all decay channels specified for that compound nucleus. The decay type defines the residual nucleus reached so that within this loop contributions from the decay of the continuum bin K to discrete levels in the residual nucleus are accumulated. Increments to the partial and total widths for the specific J $\pi$  compound nucleus state are also determined.

After the calculation is completed for decay of the continuum bin K into discrete levels in all residual systems, then the calculation for continuum to continuum transitions is made. For a given energy bin K the sum over all J $\pi$  states begins. For each compound nucleus state specified by UJ $\pi$  the sum over all decay channels (in a manner analogous to the method used for population of discrete levels) is made. For each decay process (reaction type) a sum over the allowed range of energy bins in the residual nucleus defined by the decay occurs. Within this sum contributions to both partial and total widths are obtained. Note that for both continuum-level and continuum-continuum transitions, the same methodology is used to compute decays no matter what the specific type (gamma rays, particle decay, fission).

After the calculation of partial and total widths has been completed, a series of similar loops are used to normalize each partial width by the total width for a compound nucleus state specified by UJ $\pi$ . Contributions to spectra are computed. Likewise the total population reached by any combination of decay paths needed for further compound system decays is stored. Level population arrays are also incremented. If preequilibrium corrections are made (for the first compound nucleus) then PRECMP is called. Afterwards

the loop over compound nuclei continues until all compound system decays that are energetically possible have been computed. Finally GRLINES is called to compute discrete gamma ray cross sections after cascades have occurred. These are then added to computed gamma ray spectra.

### III. Problem Setup and Execution

#### A. Input

Here a brief description of the philosophy of problem setup will be given along with information concerning additional datasets that are required. The key concern in devising the GNASH input was to keep problem-specific input as simple as possible. This was to be done while permitting maximum flexibility in terms of parameter detail that may be desired for a given problem. Additional files for input (discrete levels and transmission coefficients for example) are used which can be shared jointly among several problem types and thus do not have to be altered for each specific calculation. Tables I and II present problem setups that were covered in the computer exercises presented during the actual ICTP lectures. Two cases are given, the first being for a non fissionable nucleus ( $n + {}^{58}\text{Fe}$  at 15 and 20 MeV) while the second involves neutron reactions on  ${}^{235}\text{U}$ . References 12 and 13 provide a complete description of input options available for problem setup.

Several general comments are appropriate regarding input setup. In specifying the decay sequence for emission of particles and gamma rays from a compound system, gamma ray emission must always be first. While this is done automatically when automatic setup options are used (INPOPT = -1,1,2 or 3), this ordering must be specified manually when INPOPT=0 is specified. Also when manual setup is used (INPOPT=0) the parameters CNP(I) and CNPIP(I) must be specified. These provide information required to determine which decaying compound system and through what reaction the present compound nucleus is reached. CNPI(I) specifies the decaying compound nucleus and CNPIP(I) gives the specific reaction number involved in that compound system. Thus in the second problem setup shown involving  $n + {}^{235}\text{U}$ , the compound system  ${}^{234}\text{U}$  is reached through decay of the CN  ${}^{235}\text{U}$  (which is I=2) through neutron emission which is IR=2. Thus for  ${}^{234}\text{U}$  CNPI(3)=2 and CNPIP(3)=2.

For specification of parameters dealing with gamma ray transmission coefficient shapes and normalizations associated with the Brink Axel model, several comments are also appropriate. First of regarding the shape, EG1, GG1, EG2, GG2, G2NORM, XNFE1, EFCONM1, GDSTEP, GDELS, GDELSL, EGCON, EG3, GG3, G3NORM, and GDELE all can be used to tailor the shape to that desired for the problem at hand. These parameters are indicated schematically in Figure 9. In reality only the parameters describing the giant dipole resonance energy (EG1) and resonance width (GG1) are essential for calculation of the transmission coefficient using the Brink Axel form. However if significant detail is desired to specify the transmission coefficient shape, then XNFE1 can be set to a value greater than zero. In this case the gamma ray strength function shape can be read in from

TAPE33 ( see below) and XNFE1 then is used to specify at how many input energies strength function values will be provided. To determine the absolute normalization of the transmission coefficients as well the fraction of multipolarities desired the following procedures are used. The specification of the fraction (RE1(MP)) of a given gamma-ray polarity can be made via default values (RE1(MP)=0) or the relative strengths can be provided by the user. In this case the sum of these relative strengths over all multipolarities should equal unity. The determination of the absolute normalization of the gamma ray transmission coefficient for the MP<sup>th</sup> multipolarity is usually performed via a separate calculation in which SWS(I) is set equal to the experimental values of  $2\pi\langle\Gamma_\gamma\rangle/\langle D_0\rangle$ . Such a calculation will provide a normalization for each multipolarity used in the calculation. This value should then be used to specify GGDNORM(MP) and SWS(I) should be set negative. This procedure thus determines the appropriate normalizations for the gamma-ray strength function (see Section IV-C) which are then used for all compound systems occurring in the problem.

One final special note regarding problem input specification. If fission transition states are calculated via bandhead parameters, then the parameters EBAND, XJPBA, and PIB1 must be provided. EBAND is the bandhead energy relative to the fission barrier and XJPB band specifies the spin and parity of the bandhead member. PIB1 can be left blank in most cases but must be specified (PIB1 = -1.) when  $J^\pi = 0^-$  so that input can be properly transcribed into the appropriate spin and parity values.

As mentioned above several other input files are required. Masses and ground state spins and parities are read from TAPE13. Masses used are based upon the 1982 Wapstra mass file. Unknown spins and parities are flagged during execution. In such cases ground state spins  $J^\pi = 0^+$  (even A) and  $J^\pi = 1/2^+$  (odd A) are then used as a default in the calculation. Although discrete level data can be read from the input file, the preferred method is to read such data from TAFE8. Thus a universal library for nuclear structure data can be used in many problems. The sequence of card image types required to construct this file appears in Table 3.

Transmission coefficients for the projectile and outgoing particles are generally read in via TAPE10. We have adapted the format used by COMNUC and also now produced by SCAT for these transmission coefficients. The format is described in Ref 12. An example of a portion of a transmission coefficient file indicating the convention used for  $T_{lj}$ 's is also provided. Note that transmission coefficients for the various particles appearing in a calculation can be provided in an arbitrary order. Additionally the total, shape elastic, and reaction cross section data can be specified for each energy on the transmission coefficient grid in addition. This feature is useful in providing a complete set of cross sections in addition to those resulting from the GNASH calculations. Finally TAPE33 can be used to provide several types of additional information pertinent to a given problem. As noted above if the XNFE1 flag is set on the problem input to a value greater than zero, then an E1 gamma ray strength function shape can be provided. This shape is then normalized using the value of GGDNORM specified for the problem. If width fluctuation corrections are desired they are also provided via TAPE33. However the most common use of this file is to provide direct

reaction cross section contributions to inelastic scattering. The input description appearing in References 12 and 13 also provides instructions for formats appropriate to TAPE33. Note that when DWBA results are used to determine direct reaction contributions and these are used with reaction cross sections determined from spherical optical model calculations, the reaction cross section available for use in Hauser Feshbach or preequilibrium calculations is renormalized downward as described before. However if coupled-channel calculations are used to produce the desired transmission coefficients, then  $\sigma_{CN} = \sum_l T_l^{CC} = \sigma_R - \sigma_D$ . Therefore no renormalization is necessary. In this case NLDIR in the input should be flagged as NLDIR+100 to indicate no renormalization is appropriate.

## B. Output

Again details concerning problem output were provided in the computer exercises and sample problem outputs were provided along with the preliminary GNASH ICTP lecture notes<sup>14</sup>. Output expected from a given problem run will occur in 5 main parts. The first part provides a list of the input as well as a description of the decay chains and other data determined from problem setup. For fission problems a detailed listing of fission barrier and transition state parameters determined from the input are given. Secondly if direct reaction data is provided, such cross sections interpolated at the particular incident energy are listed. Then preequilibrium output is provided which is followed by renormalized Hauser Feshbach calculations appropriate for the first compound system. Binary reaction and preequilibrium summary data then occur. (Note that the preequilibrium normalizations listed have no real meaning for the present code version.)

This begins the main part of the output data. It is followed by data from individual reactions in which level decay, level excitation, and total production cross sections are given. Spectra resulting from the decays from the specified compound nuclei are also provided. It is within this portion that cross sections for specific reaction paths can be determined. To do so all particle paths leading to a specific compound nucleus must be summed together. From this sum, cross sections for further decay by particle emission or fission must be subtracted to obtain the desired cross section. Note that if gamma decay of the residual nucleus produced by the reaction of interest is included in the calculation, then summation of the yield of the ground state and any long-lived isomeric states (which are listed in the discrete level section) should provide a similar cross section value. This holds true if there are enough multipolarities included in the calculation in order to prevent trapping of cross section in the continuum. Following the section dealing with cross sections and spectra for individual reaction paths are similar data for composite spectra produced by summing contributions over all reaction paths occurring in the calculation (if IPRTSP=3 or 1). In this instance particle emission cross sections have multiplicities included. Note that all spectra are angle integrated and spectra from individual reactions are given in the center of mass system of the recoiling nucleus plus particle or gamma ray. Fission "spectra" have no real meaning.

Following these spectral data are discrete level cross sections computed for both particle and gamma ray emission (assuming  $IPRTLEV=1$ ). Finally if  $IPRTGC=1$ , information is provided for level density parameters appropriate for all nuclei appearing in the calculation.

## SECTION III - CURRENT DEVELOPMENT

### I. Introduction

In this final section, a brief description of current developments underway in the GNASH code will be given. These are meant to improve the models used in the code as well as to increase capabilities for higher energy calculations. The areas that will be briefly addressed are (1.) implementation of an evaporation model with a full treatment of gamma ray competition to particle emission; (2.) implementation of an "s-wave" approximation to the Hauser Feshbach formalism; (3.) multistage preequilibrium emission within the exciton model framework; (4.) implementation of the Ignatyuk level density model; and (5.) development of capabilities for calculation of angle-dependent particle emission spectra.

### II. Evaporation and S-Wave Approximation Models

The evaporation model implemented in GNASH is based upon the formalism of Buttner<sup>14</sup>. The same structure used in the code for standard Hauser Feshbach calculations has been retained so that partial widths for continuum-continuum transitions involving particle emission are calculated using the expression

$$\Gamma_b = (2s_b + 1) \int_{E_{\min}}^{E_{\max}} d\epsilon \left[ \sum_{\ell} (2\ell + 1) T_{\ell}(\epsilon) \rho(E_{\max} - \epsilon) \right] \quad (35)$$

A similar contribution is calculated for continuum-level transitions except in this case only transmission coefficient sums evaluated at the exit particle energy involved in the transition appear. This procedure ignores effects due to the spin, parity of the levels involved. For gamma rays a similar form is used

$$\Gamma_{\gamma} \propto \frac{2}{\pi} \frac{1}{\hbar^2 c^2} \int_{E_{\min}}^{E_{\max}} d\epsilon_{\gamma} \epsilon_{\gamma}^2 \sigma_{\gamma} \rho(E_{\max} - \epsilon_{\gamma}) \quad (36)$$

where since only E1 radiation is included, the photoabsorption cross section  $\sigma_{\gamma}$  is determined from giant dipole resonance data.

The implementation of this evaporation version has allowed practical calculations at higher projectile energies, since runing times are significantly smaller. Additionally the code has been modified to include the decay of up to 70 compound systems in one calculation and from each compound nucleus n,p,d,t, $\alpha$ , and  $\gamma$  emission are automatically included. Thus

cross sections for up to 420 reaction paths can be determined in one calculation. To facilitate problem setup, the input has been greatly simplified so that the user has only to specify ranges in  $\Delta N$  and  $\Delta Z$  from the target over which the reaction sequence will be computed.

Concurrent with this evaporation model development is the implementation of an approximation to standard Hauser-Feshbach theory known as the "s wave approximation<sup>15</sup>". In this model the standard Hauser Feshbach cross section expression

$$\frac{d\sigma}{d\epsilon_b} = \frac{\pi}{k^2} \sum_{l=0}^{\infty} (2l+1) T_l (2s_b + 1) \sum_{\ell=0}^{\infty} T_b^{\ell}(\epsilon) \sum_{J=|l-\ell|}^{l+\ell} \frac{\rho(E,J)}{D} \quad (37)$$

is replaced with

$$\frac{d\sigma}{d\epsilon_b} = \frac{\pi}{k^2} \sum_{l=0}^{\infty} (2l+1) T_l (2s_b + 1) \sum_{\ell=0}^{\infty} (2\ell+1) T_b^{\ell}(\epsilon) \frac{\rho(E,l)}{D} \quad (38)$$

Here  $T_l$  is the transmission coefficient for the  $l^{\text{th}}$  partial wave of the projectile,  $\rho(E,J)$  is the level density for the residual nucleus, and  $D$  is the total width obtained by integrating over all emission energies and exit channels. In going from (37) to (38) the assumption is made that  $\rho(E,J)$  can be replaced with  $\rho(E,l)$  which means that the spin distributions in both the compound and residual systems are the same. The spin distribution in the initial compound system is determined by the standard sum over incident channel transmission coefficients available from an optical model calculation. This spin distribution is then projected unchanged throughout the problem.

A main motivation for implementation of this approach is the development of a fast and reliable method for gamma ray production calculations at high projectile energies. Figure 10 illustrates that for the case of 50 MeV  $n + {}^{56}\text{Fe}$  reactions, the s-wave approximation produces results that are similar to those from a full Hauser Feshbach calculation. For evaporation calculations using the methods described above, the results obtained are lower, and many of the features which result from discrete gamma-ray lines are absent. The underprediction of gamma production cross sections obtained from an evaporation calculation persists until incident energies around 60 MeV are reached. Fig 11 illustrates this point. Finally Fig 12 illustrates gamma ray production cross sections calculated using this method to data for  $n + \text{Ta}$  reactions measured by Gould and Wender (personal communication 1987) between 20 and 80 MeV.

### III. Nuclear Level Density Model Development

The description of nuclear level densities at high excitation energies presents a



major problem in statistical model calculations. Such difficulties are complicated by the effect of shell closures on the Fermi gas parameter and their propagation to higher energies. A method for addressing them is use of the model developed by Ignatyuk<sup>16</sup> which has now been implemented in GNASH. This model assumes the Fermi gas parameter  $a$  to be energy dependent in contrast to the assumption of the other level density models discussed in these lectures. Thus  $a=a(U)$  which is given by

$$a(U) = a \{1 + f(U)\delta W/U\} \quad (39)$$

where  $a$  is the asymptotic value for the Fermi gas parameter occurring at high energies. Shell effects are included in the term  $\delta W = M_{\text{exp}}(Z,A) - M_{\text{ld}}(Z,A,\alpha)$  where  $\alpha$  is the deformation. This term is evaluated in GNASH using the Wapstra 1982 mass compilation along with standard liquid drop mass results calculated at the deformation  $\alpha$ . The term  $f(U)$  provides the energy dependence and is  $f(U) = 1 - \exp(-0.05U)$ . Finally the asymptotic form of  $a$  was fit as a function of mass. The following result was obtained

$$a/A = 0.1375 - 8.36 \times 10^{-5} A. \quad (40)$$

This model thus permits shell effects to be included at low excitation energies while at higher energies such effects disappear as  $a(U)$  approaches the asymptotic value of  $a$ . This result is in better agreement with results obtained from microscopic level density calculations. Fig 13 compares the  $^{208}\text{Pb}$  total level density calculated with this model to results obtained from the Gilbert Cameron model.

#### IV. Multistage Preequilibrium Emission

At higher projectile energies there is an increasing probability that after preequilibrium emission has occurred within the target nucleus, residual systems still have enough excitation energy to emit particles in a preequilibrium phase rather than through an equilibrium process. This situation can be handled straightforwardly within the excitation model discussed earlier by changing the initial conditions to

$$P_0^* (n^* = n-b) = W_b(n, \epsilon_b) \tau(n, E) \quad (41)$$

In GNASH for such multistage contribution calculations, the master equations are not solved in detail, but the assumption is made that only transitions of the type  $n \rightarrow n+2$  ( $\lambda^+$ ) are important. Thus closed form expressions can be determined for the angle-integrated preequilibrium cross section contributions. The multistage preequilibrium cross section is then computed using

$$\frac{d\sigma}{d\epsilon_{b'}} = \sigma_{CN} \sum_{n^*=n_0}^6 W_{b'}(n^*, \epsilon) \tau(n^*, E^*) D(n^*) \quad (42)$$

The initial exciton numbers extend from 2 to 6 and the sums in the residual systems extend to  $n_0^* + 6$ . The mean lifetime and depletion factors appearing in Eq (42) are given respectively by

$$\tau(n^*, E^*) = \frac{W_b(n, \epsilon_b) \tau(n, E)}{\lambda^+(n^*, E^*) + \sum_{b'} \int_{E_{\min}}^{E_{\max}} W_{b'}(n^*, \epsilon) d\epsilon} \quad (43)$$

$$D(n^*) = \prod_{n'=n_0}^{n^*-1} [1 - \tau(n', E^*) \sum_{b'} \int_{E_{\min}}^{E_{\max}} W_{b'}(n', \epsilon) d\epsilon]$$

where  $E^* = E - B - \epsilon_b$ . Preequilibrium components are calculated for  $\Delta Z=0,1$  and  $\Delta N=1,0$  from the Z and N of the target system. Figure 14 illustrates the effect on a calculated 90 MeV p +  $^{27}\text{Al}$  neutron emission spectrum. Although the effects are not large with respect to total emission spectra for these energies, the yields of specific residual nuclei occurring in the calculation can be significantly affected for incident energies greater than about 50 MeV.

## V. Angle Differential Spectra

Two methods have been developed to calculate angle dependent spectra in GNASH. The first uses an extension<sup>2</sup> of the Kalbach-Mann systematics<sup>17</sup> to determine the angular distribution of continuum particle emission. In this new extension the Legendre coefficient expansion associated with the previous systematics was replaced with an exponential in  $\cos\theta$ . The resulting expression developed by Kalbach and implemented in GNASH is

$$\frac{d^2\sigma}{d\Omega d\epsilon_b} = \frac{1}{4\pi} \frac{d\sigma}{d\epsilon_b} \frac{a}{\sinh(a)} [\cosh(a\cos\theta) + f_{MSD} \sinh(a\cos\theta)] \quad (44)$$

where  $f_{MSD}$  represents the cross section portion occurring through multistep direct processes (ones involving unbound p-h configurations). In GNASH this quantity is assumed

equal to the total preequilibrium cross section resulting from interaction with the target nucleus. Once this choice of parameterization in terms of  $\cos\theta$  was determined, a straight line fit was made versus  $\cos\theta$  to extract a slope parameter. Kalbach found that such slopes exhibited a systematic behavior which depended most strongly upon the outgoing channel energy of the emitted particle. This behavior is illustrated in Fig 15 where slopes determined from the analysis of (p,p'),(p,d), and ( $\alpha,\alpha'$ ) data on  $^{56}\text{Fe}$  are shown.

The second method for angular distribution calculations is based upon the generalization of the exciton preequilibrium model using a free scattering kernel as developed by Akkermans, Gruppelaar, and Reffo<sup>18</sup>. Generalization of the exciton preequilibrium model results in the replacement of the expression for the mean lifetime  $\tau(n,E)$  with  $\tau(n,E,\Omega)$  as follows

$$\tau(n,E,\Omega) = \tau(n,E) Q(n,\Omega) \quad (45)$$

where

$$Q(n,\Omega) = \sum_{\ell} (\mu_{\ell})^{(n-n_0)/2} \mathcal{X}_{\ell}(n_0) P_{\ell}(\cos\theta) \quad (46)$$

Here  $\mu_{\ell}$  are eigenvalues for this equation and  $\mathcal{X}_{\ell}$  is defined as

$$\mathcal{X}_{\ell}(n_0) = \delta_{n,n_0} \frac{(2\ell+1)}{4\pi} \mu_{\ell} \quad (46a)$$

$P_{\ell}$  are Legendre coefficients. If Legendre coefficients from  $\ell=0$  to 4 are included then the double differential emission spectrum can be obtained from

$$\begin{aligned} N_b(\varepsilon,\Omega) = & \frac{\sigma_{CN}}{4\pi} \sum_n W_b(n,\varepsilon) \tau(n,E) \left\{ 1 + 2\left(\frac{2}{3}\right)^{(n-n_0)/2} \cos\theta \right. \\ & + \frac{5}{4}\left(\frac{1}{4}\right)^{(n-n_0)/2} \left(\frac{3}{2} \cos^2\theta - \frac{1}{2}\right) \\ & \left. - \frac{3}{8}\left(-\frac{1}{24}\right)^{(n-n_0)/2} \left(\frac{35}{8} \cos^4\theta - \frac{15}{4} \cos^2\theta + \frac{3}{8}\right) \right\} \end{aligned} \quad (47)$$

Fig 16 compares angular distributions calculated using these two approaches to the 90 MeV  $^{27}\text{Al}(p,xn)$  data of Kalend<sup>19</sup> for an emission energy of 20 MeV. Here both models provide a good representation of the data. However the free scattering kernel is applicable primarily at higher incident energies since effects due to the nuclear medium are not included. At lower incident energies this model fails to reproduce cross sections occurring at backward emission energies.

The combination (and implementation) of these models have produced the GNASH code system which is illustrated in Fig 17. As discussed before a variety of reaction models are available for use in calculations covering a wide incident energy range. Angular distributions are available using the methods described above. Finally auxiliary codes exist for formatting of GNASH-calculated data into the new ENDF File6 format and for determining thick target spectral yields for incident charged-particle reactions.

## REFERENCES

1. C. Kalbach, Zeits. fur Physik A**283**,401(1977).
2. C. Kalbach, "Systematics for Continuum Angular Distributions: Extension to Higher Energies" Los Alamos National Laboratory report, LA-UR-87-4139 (1987).
3. A. Gilbert and A.G.W. Cameron, Can. J. Physics **43**,1446(1965).,
4. W. Dilg,W. Schantl, H. Vonach, and M. Uhl, Nucl Phys A**217**,269(1973).
5. J. L. Cook, H. Ferguson, and A.R. de L. Musgrove, Aust. J. Phys. **20**, 477(1967).
6. J. M. Blatt and V. Weisskopf, Theoretical Nuclear Physics (John Wiley and Sons, Inc., New York, 1952).
7. P. Axel, Phys. Rev. **126**, 671(1962).
8. C. Kalbach, " PRECO Program for Calculating Preequilibrium Particle Energy Spectra", Saclay Report DPh-N/BE/74/3(1974).
9. C. Kalbach, Phys. Rev. C**32**, 1157(1985).
10. C. Kalbach, "PRECO-D2: Program for Calculating Preequilibrium and Direct Reaction Double Differential Cross Sections", Los Alamos National Laboratory report LA-10248-MS (1985).
11. A. Jensen, "Recent Developments in the Theory of Nuclear Level Densities", Proceedings Int. Conf. on Neutron Physics and Nuclear Data, Harwell, p.378(1978).
12. P. G. Young and E. D. Arthur,"GNASH: A Preequilibrium, Statistical Nuclear Model Code for Calculation of Cross Sections and Emission Spectra", Los Alamos National Laboratory report, LA-6947 (1977).
13. E. D. Arthur, "The GNASH Preequilibrium Statistical Model Code", Los Alamos National Laboratory report, LA-UR-88-382(1988).
14. H. Buttner, A. Lindner, H. Meldner, Nucl. Phys. **63**, 615 (1965).
15. M. Blann and M. Beckerman, Nucleonika**23** , 1(1978).
16. A. V. Ignatyuk, G. N. Smirenkin, and A. S. Tishin, Sov. J. Nucl. Phys. **21**, 255(1975).
17. C. Kalbach and F. Mann, Phys. Rev. C**23**, 112(1981).
18. J. Akkermans, H. Gruppelaar, and G. Reffo, Phys. Rev. C**22**,73(1980).
19. A. M. Kalend et al, Phys. Rev. C**28**, 105(1983).

Table 1

n + <sup>58</sup>Ni Problem Input

1	n + ni58	vax	gnash	test																
2	1-15-88																			
3	1	0	0	3	1	1														Print flags
4	-1	0	0	0	0	17														Input setup option flag, no of direct levels read from TAPE33
5	5	2	2	1																No of CN, no of gamma ray multipolarities, gamma ray TC option, preeq flag
6	1.		28058.			1.0														Target specification
7	2																			No of incident energies
8	15.		20.																	Incident energies
9	28059.		4.			-.1			1.			1001.	2004.							1st CN decays
10	28058.		4.			-.1			1.			1001.	2004.							2nd CN decays
11	27058.		3.			-.1			1.			1001.								3rd CN decays
12	27057.		3.			-.1			1.			1001.								4th CN decays
13	26055.		2.			-.1			1.											5th CN decays
14		e1	.82			.12														E1 fract and norm
15		m1	.18			.008														M1 fract and norm
16		19.0	5.5																	GDR shape parameters
17		0.0																		
18		1.6	4.538																	Preequilibrium norm and composite system state density

\*



38	6.	6.4		Begin barrier parameters 235U
39	.85	.55		
40	10.	2.		
41	-1.			
42	4			
43	0.	.5		Begin 235U transition state data for barrier A
44	.047	-3.5		
45	.054	-2.5		
46	.114	5.5		
47	4			
48	0.	.5		Transition state data barrier B
49	.009	1.5		
50	.026	-3.5		
51	.183	-2.5		
52	6.4	5.8		Begin barrier parameters 234U
53	1.2	.8		
54	2.	2.		
55	-1.			
56	3			
57	0.	0.	1.	Transition state data barrier A
58	.6	2.		
59	1.	-1.		
60	3			
61	0.	0.	1.	Transition state data barrier B
62	.6	2.		
63	1.	-1.		

\*



## Discrete Level File Input Parameters

For each residual nucleus requiring discrete level data the following card sequence is required. Note that the essential parameters that must be specified are ID, NL, NX, EL(N), AJ(N), NT, NF, P, and CP. The other values may be left blank.

- (A) (1 card) FORMAT (I8, I5, F12.6): ID, NL, F  
 (B) Outer loop on levels (DO loop N = 1, NL)  
     FORMAT (I6, F12.6, 2F6.1, E12.5, I6): NX, EL(N), AJ(N), AT(N), TAU, NT  
 (C) Inner loop for each level (DO loop K = 1, NT)  
     FORMAT (I2X, I6, 2F12.6): NF, P, CP

<u>Parameter</u>	<u>Description</u>
ID	1000 * Z + A of the nucleus whose levels are being input.
NL	Number of levels being input.
F	For card input, set F = -1. for the last nucleus (highest ID) for which level data is input. Otherwise, set F = 0.
NX	Level number (= N), that is, N = 1 for the ground state, N = 2 for the first excited state, etc.
EL(N)	Energy in million electron volts of the Nth level; that is, EL(1) = 0.
AJ(N)	Spin and parity of the Nth level. The sign of AJ(N) indicates the parity. For example, -0. is interpreted as a $J^\pi = 0^-$ state.
AT(N)	Isospin of the Nth level (if unknown, it is set equal to 99.0). AT(N) is not used in the calculation at present.
TAU	Half-life of the state in seconds (if unknown, it is set equal to 99.0 or 0.0). TAU is not used in the calculation.
NT	Number of gamma-ray branches from the Nth level to lower levels.
NF	Level number indicator for a level to which a gamma-ray transition is occurring.
P	Gamma-ray branching ratio for the transition defined by $N \rightarrow NF$ . For bound states, $\sum_{NF} P(N \rightarrow NF) = 1$ . For unbound states, $\sum_{NF} P(N \rightarrow NF) =$ the total probability for decays other than particle emission.
CP	Probability that the transitions characterized by $P(N \rightarrow NF)$ are gamma-ray transitions. If, for example, there is a 20% probability that electron conversion is the decay mechanism, then CP = 0.80.

## FIGURES

1. Decay sequence for GNASH  $n + {}^{64}\text{Zn}$  calculation.
2. GNASH input files and output capabilities.
3. Schematic of decay sequences.
4. Residual nucleus specification by discrete levels and a continuum excitation energy region.
5. Method for calculation of decays from a given compound system.
6. Representation of fission "decay" in GNASH.
7. GNASH structure.
8. SPECTRA subroutine logic.
9. Schematic representation of gamma-ray transmission coefficient shapes within the Brink Axel model.
10. A comparison of gamma-ray production spectra resulting from 50 MeV  $n + {}^{56}\text{Fe}$  reactions as calculated using the Hauser Feshbach model, "s-wave" approximation, and evaporation model.
11. Total gamma-ray production calculated using the same three models.
12. A comparison of the gamma-ray production cross section calculated using the evaporation model to the data of Wender and Gould for  $n + \text{Ta}$  reactions between 20 and 80 MeV.
13. The  ${}^{208}\text{Pb}$  level density calculated using the Ignatyuk and Gilbert Cameron models.
14. A comparison of 90 MeV  ${}^{27}\text{Al}(p,xn)$  emission spectrum calculated with and without multistage pre-equilibrium emission to the data of Kalend.
15. Angular distribution slope parameters determined by Kalbach from analysis of particle reaction data for  ${}^{56}\text{Fe}$ .
16. A comparison of the angular distributions for 20 MeV neutron emission resulting from 90 MeV  $p + {}^{27}\text{Al}$  reactions calculated using the Kalbach angular distribution systematics with that using the free scattering kernel within the exciton model.
17. A schematic representation of the current GNASH nuclear model code system.

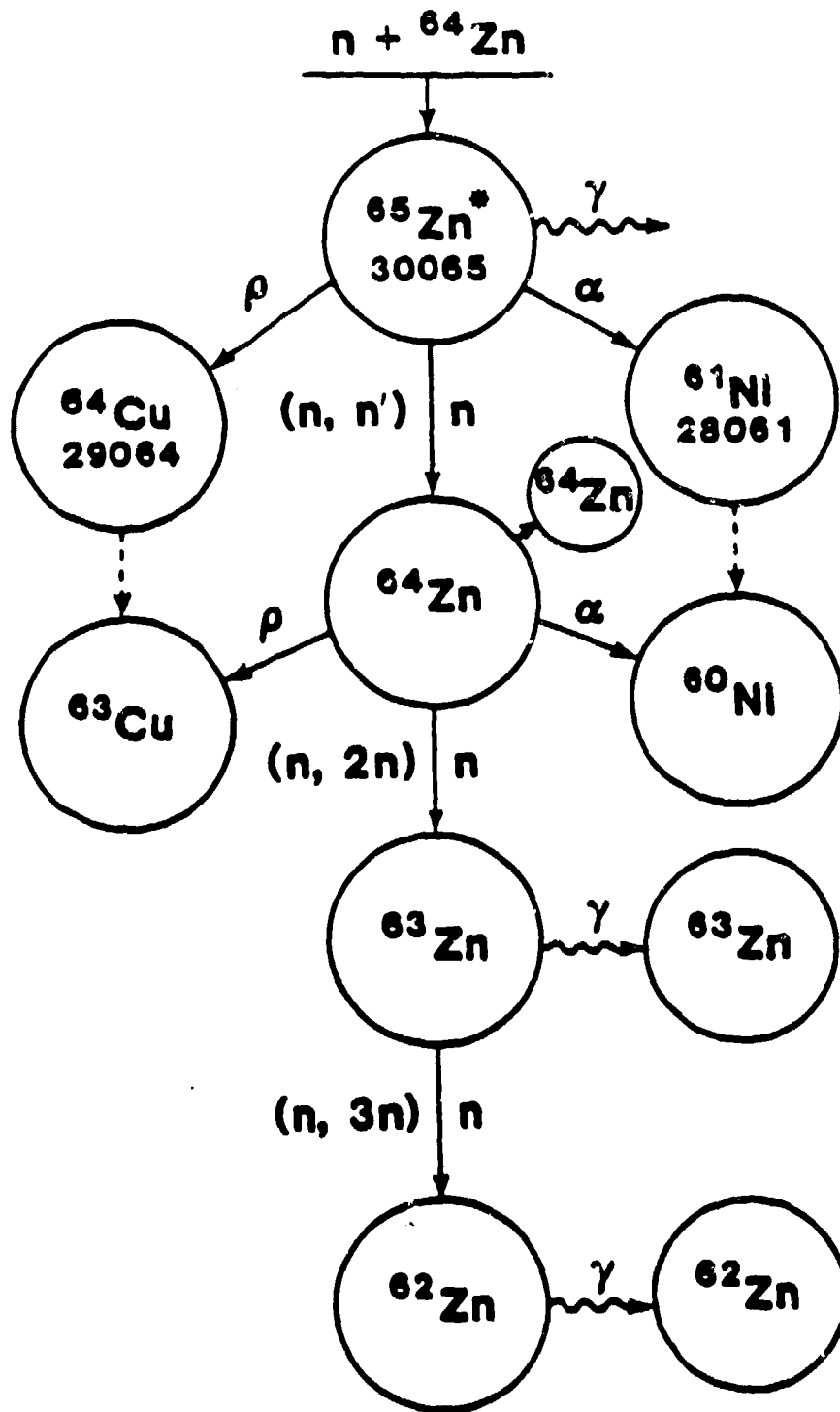


Fig 1

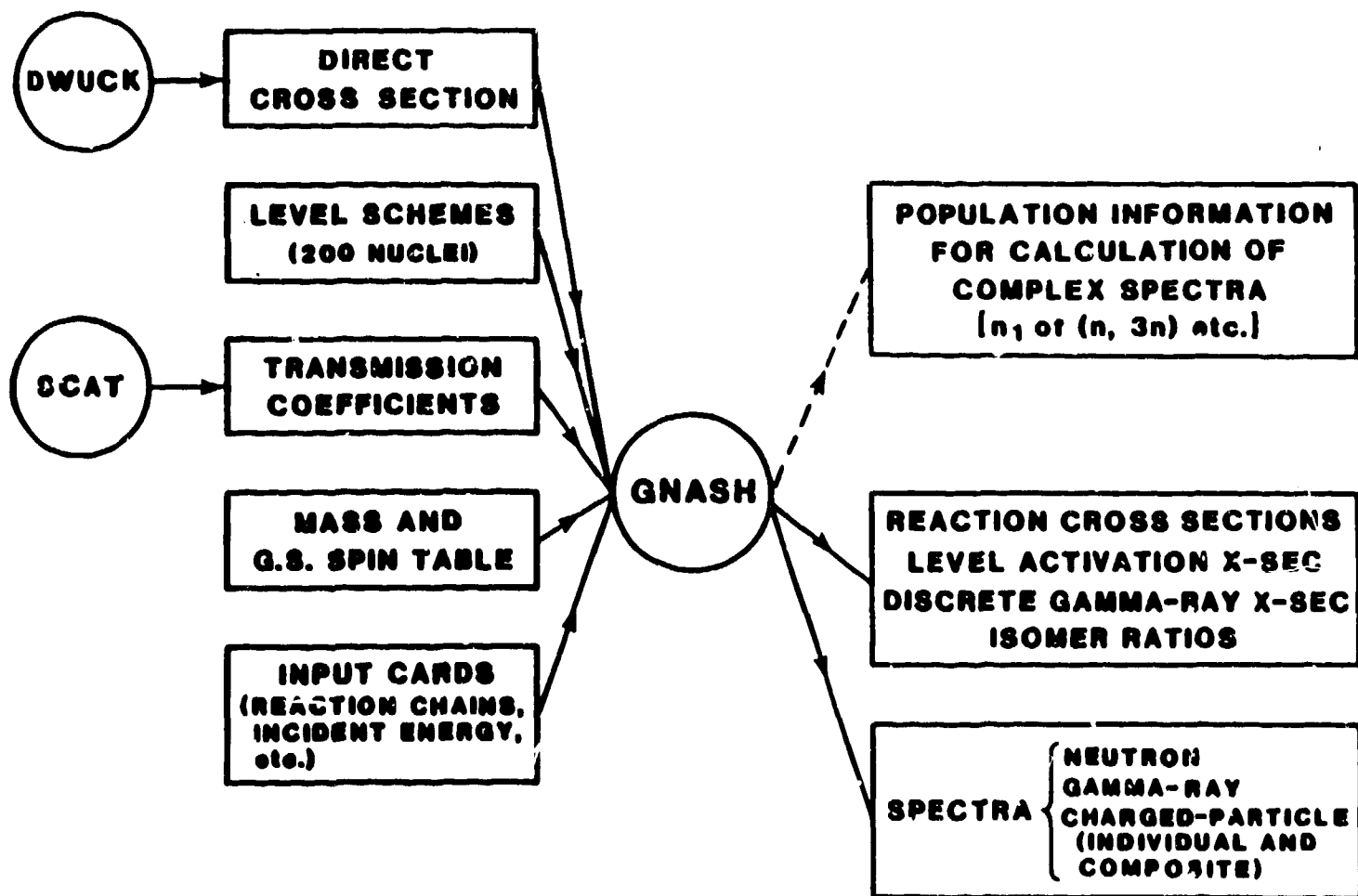


Fig 2

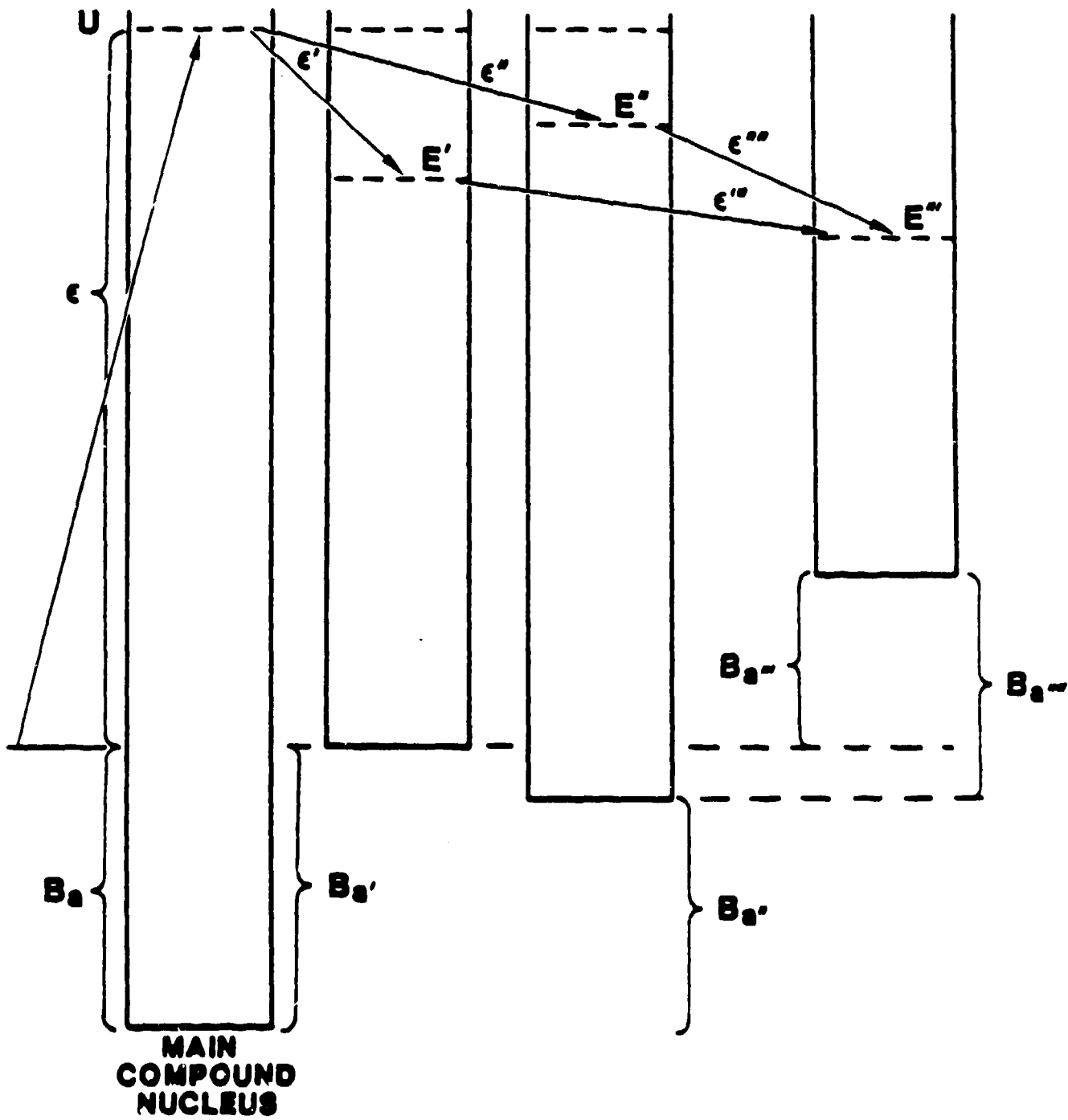


Fig 3

FIG 4

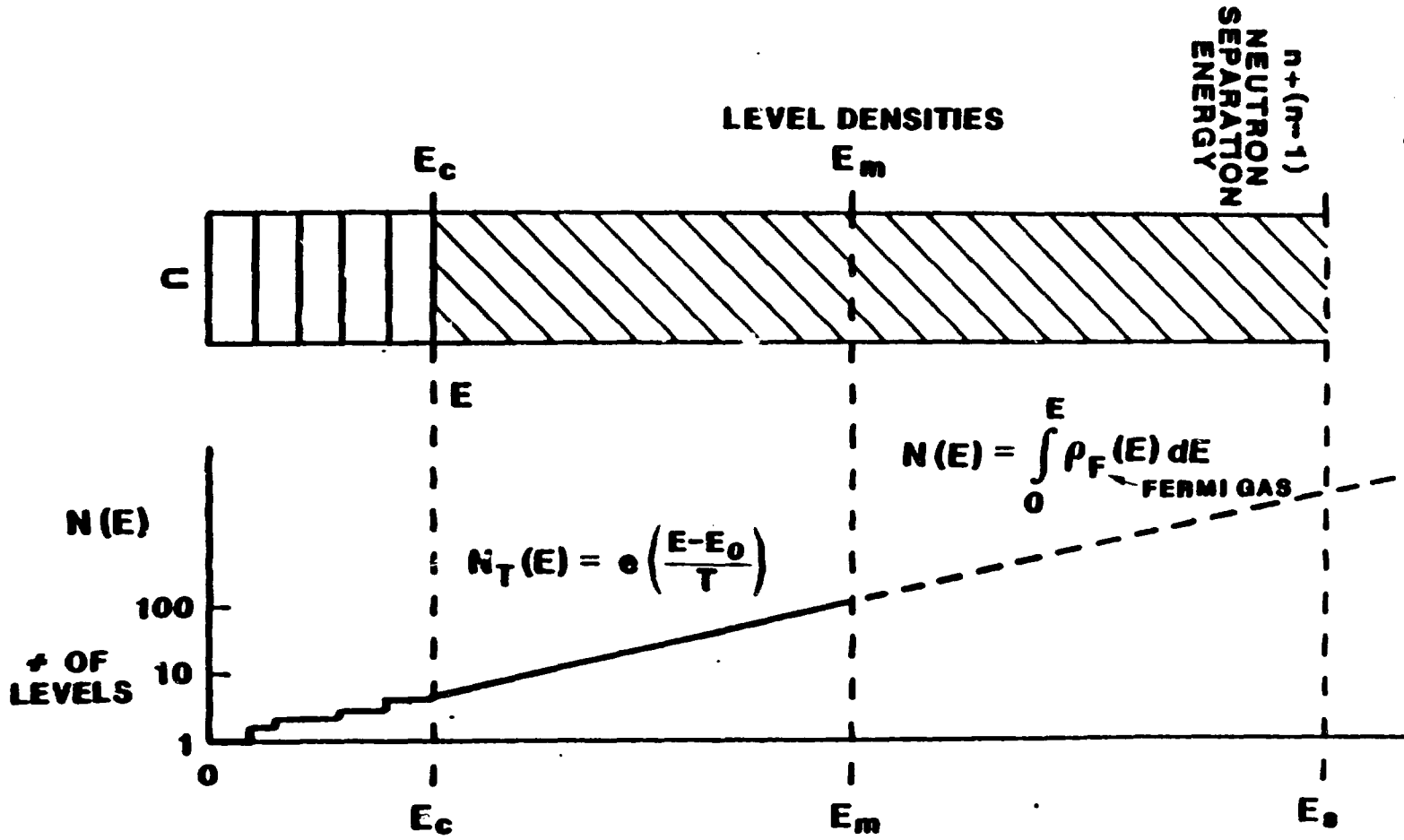
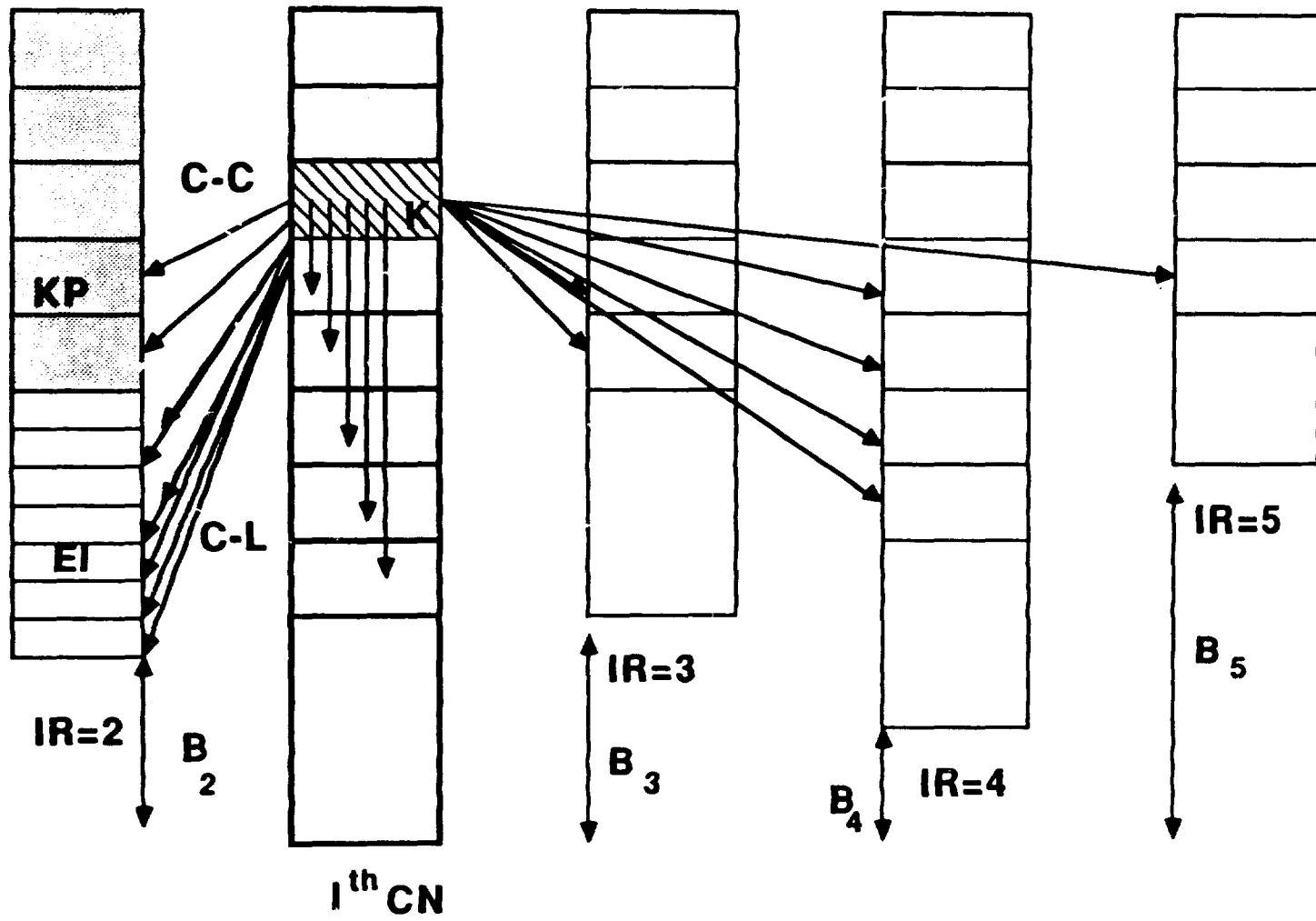


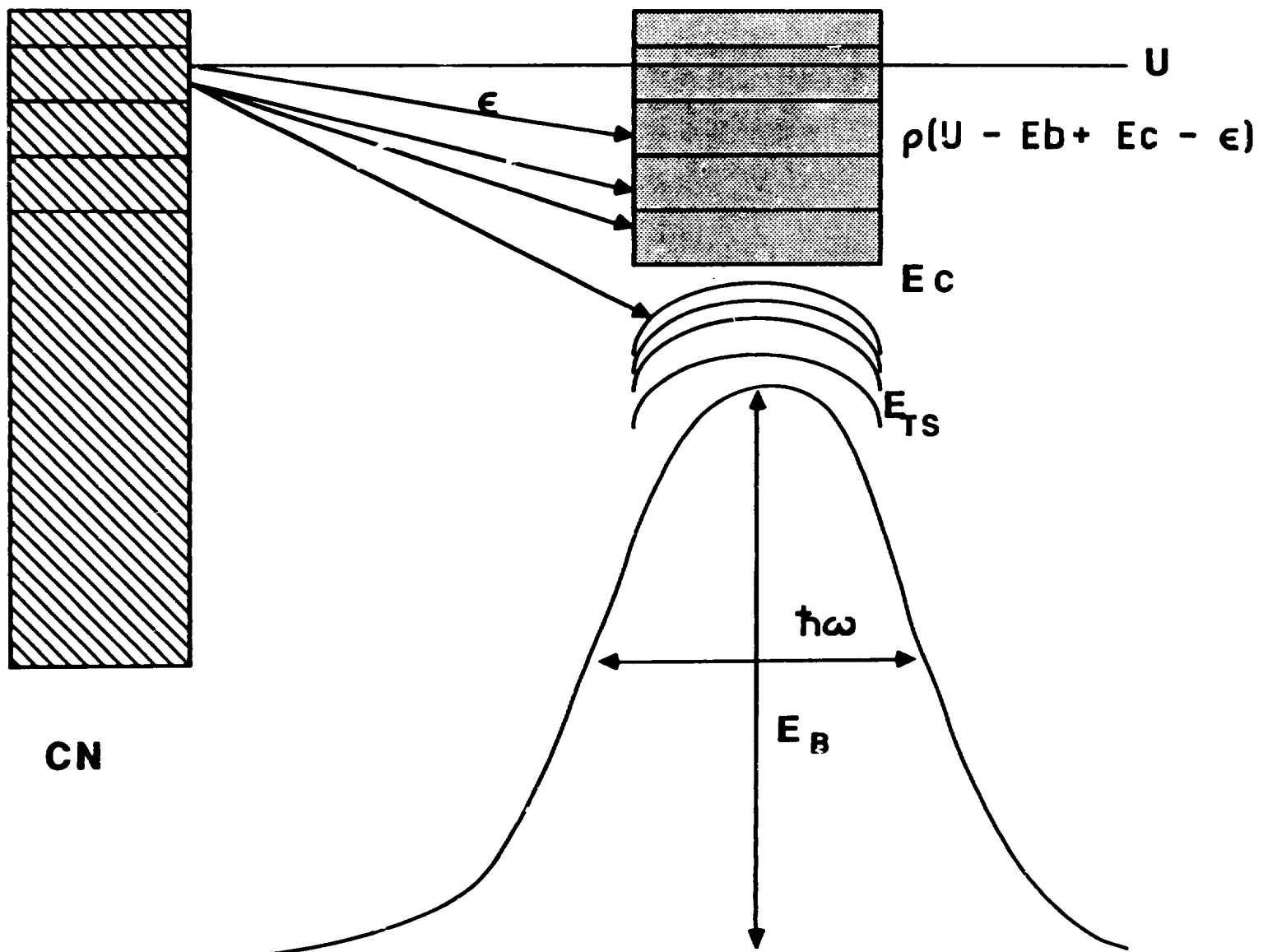
Fig 5



$I^{\text{th}} \text{CN}$   
(IR=1)

C-C:  $DP = P(K) T(\epsilon) \rho(U') d\epsilon$   
 C-L:  $DL = P(K) T(U-EI)$

Fig 6





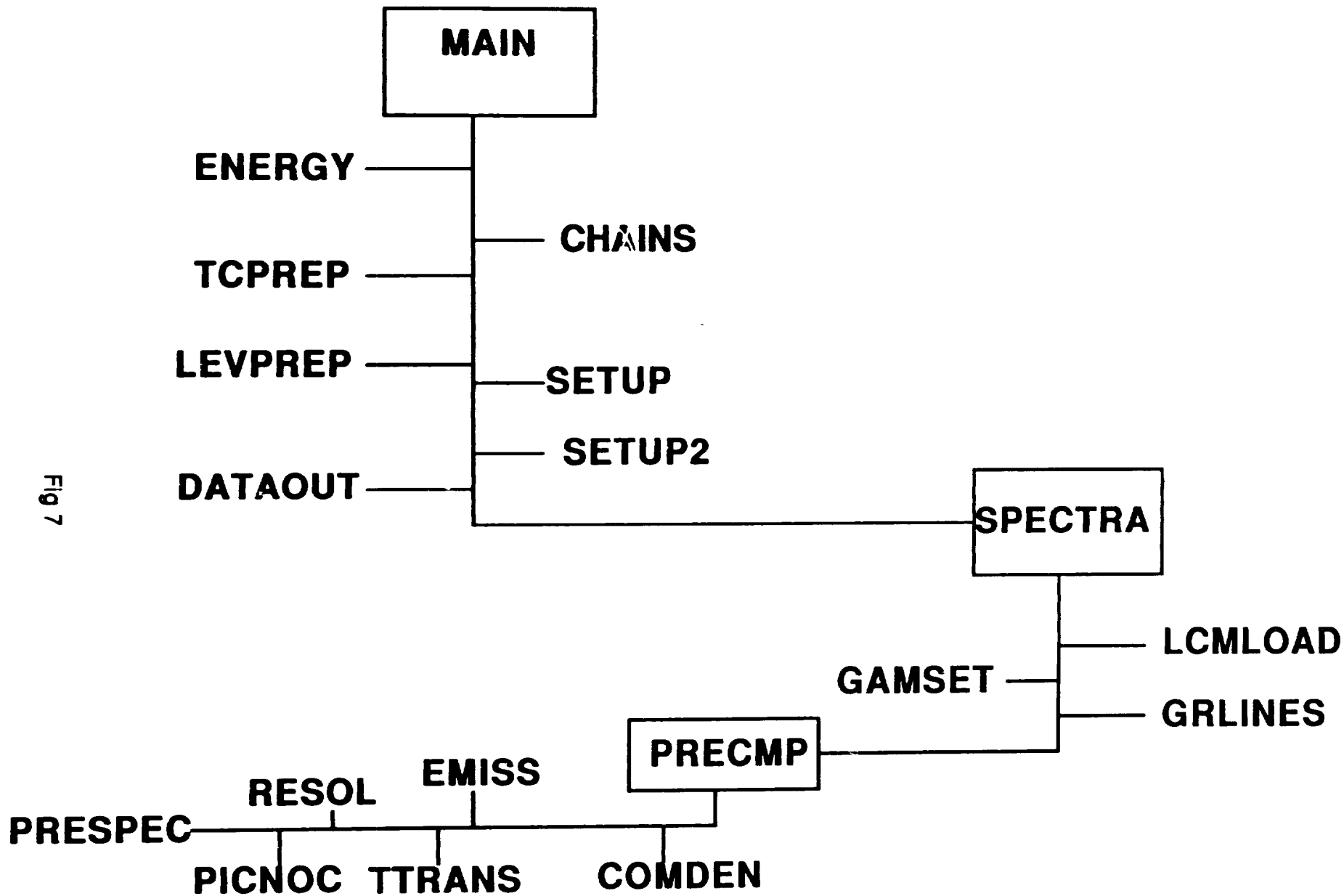


Fig 7

Do 400 K=1,NKCN For lth CN begin loop on energy bin K  
 Do 301 IP=1,NIP For each K bin loop over possible decay channels  
 Do 280 N=1,NLEV2 For each residual system loop over discrete levels  
     Accumulate populations and increment total width sum  
     (gamma-ray and particle emission, fission)  
 End N and IP loops

Initial Continuum-  
Level Transition  
Calculation

Do 300 IP=1,NIP Loop over possible decays  
 For a CN state of E, spin, and parity loop over l and  
 s sums  
 Do 180 KP = KLOW,KUP For a given K and IR, loop over  
     all continuum bins available in the residual system  
     Accumulate populations for continuum-continuum transitions  
     and increment total width sum  
 END IP, spins, and KP loops

Initial Continuum-  
Continuum Transition  
Calculation

Total width  
calculation completed,  
all population increments obtained

Do 851 IP=1,NIP Sum over possible decays  
 Do 695 KP= KLOW,NK2 Loop over continuum bins in residual system  
     Normalize populations for continuum-continuum  
     transitions by total width, accumulate spectral contributions  
     Store populations needed for subsequent CN's  
 END KP loop  
 Do 800 N=1,NLEV2 Loop over levels in each residual system  
     Normalize level population increments by total width  
     Add into spectra  
 END N loop  
 END loop over decays  
 END compound nucleus K loop  
 END loop over decaying CN

Normalize all  
populations by total  
width

Fig 8

FIG 9

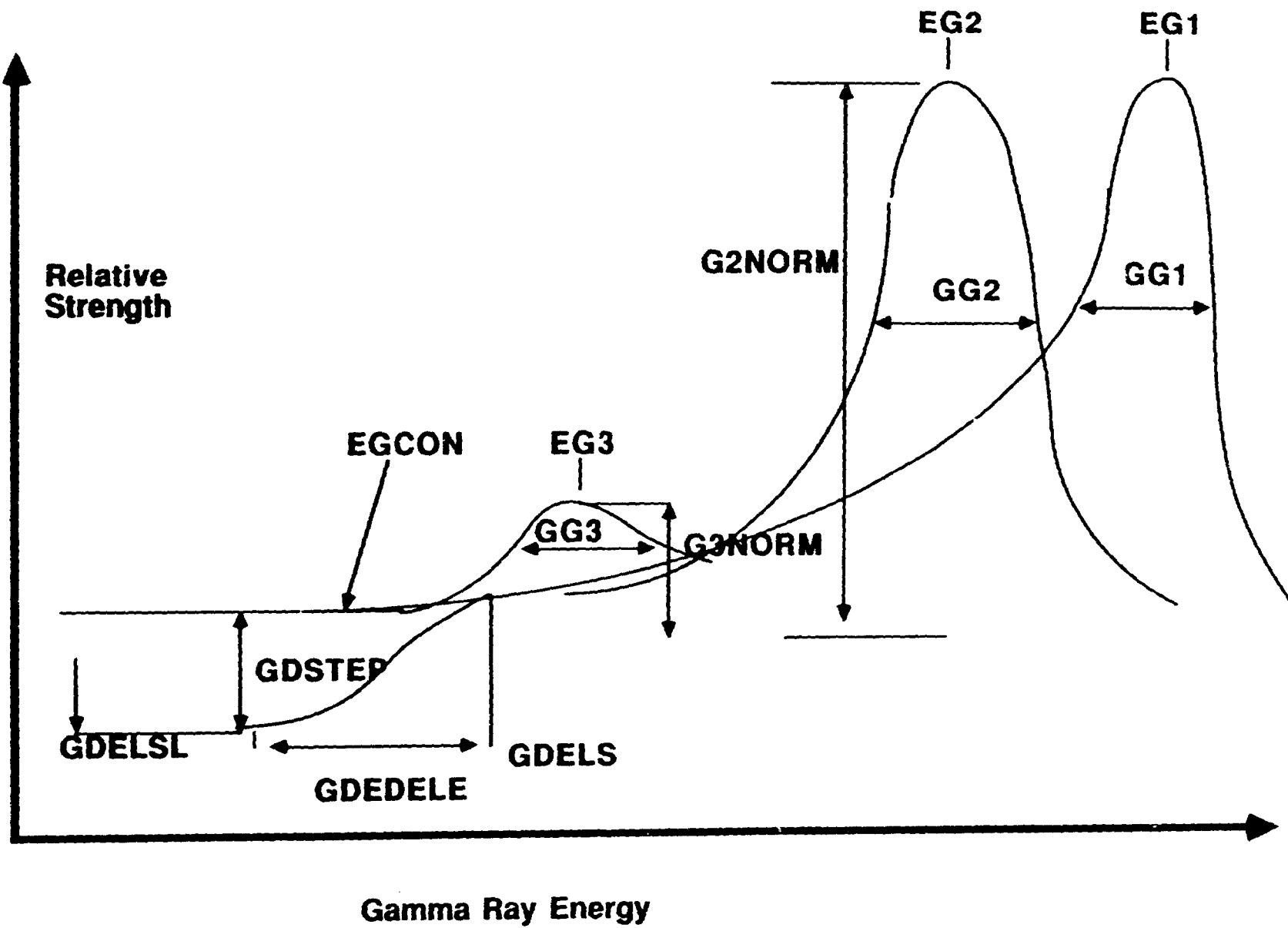


Fig 10

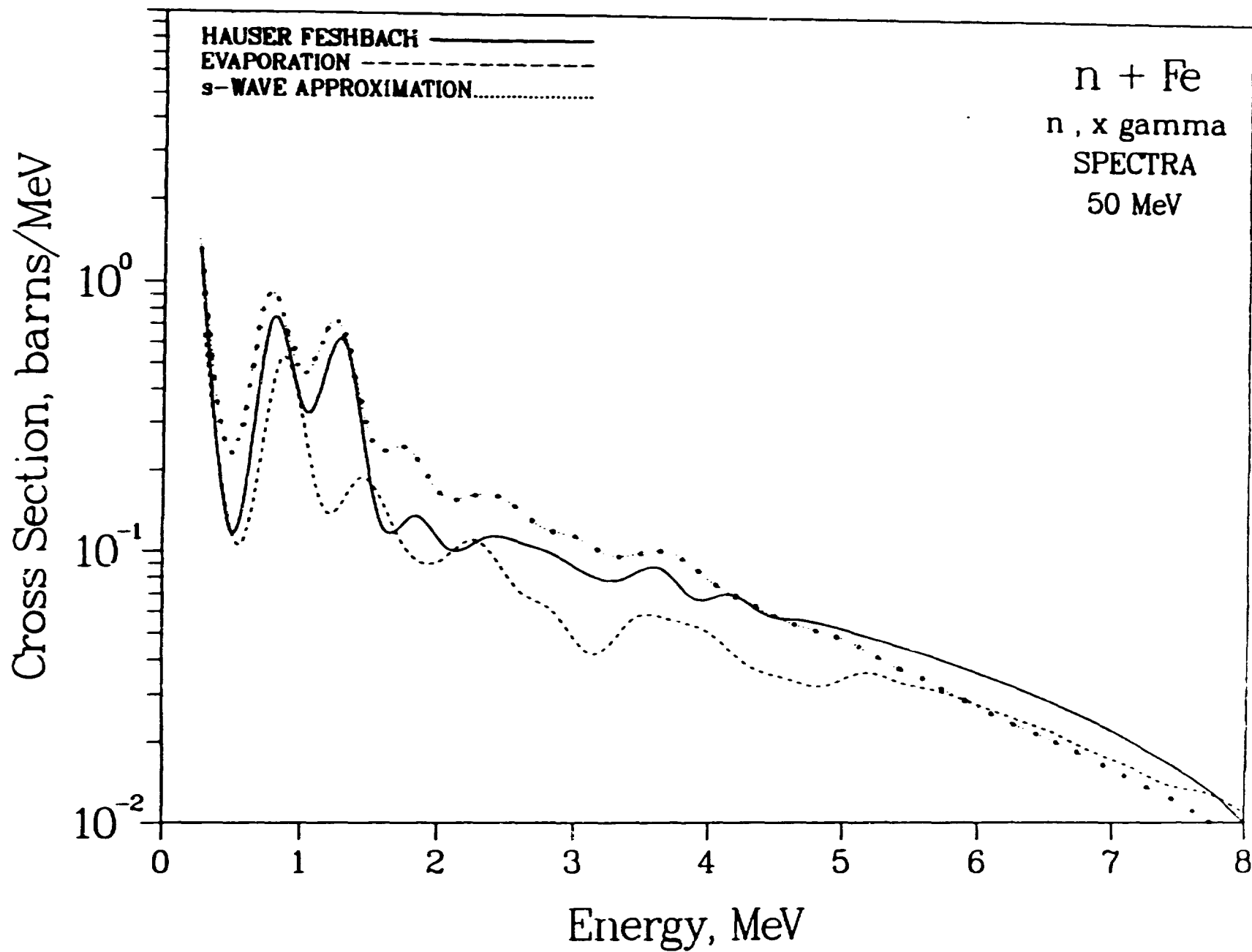
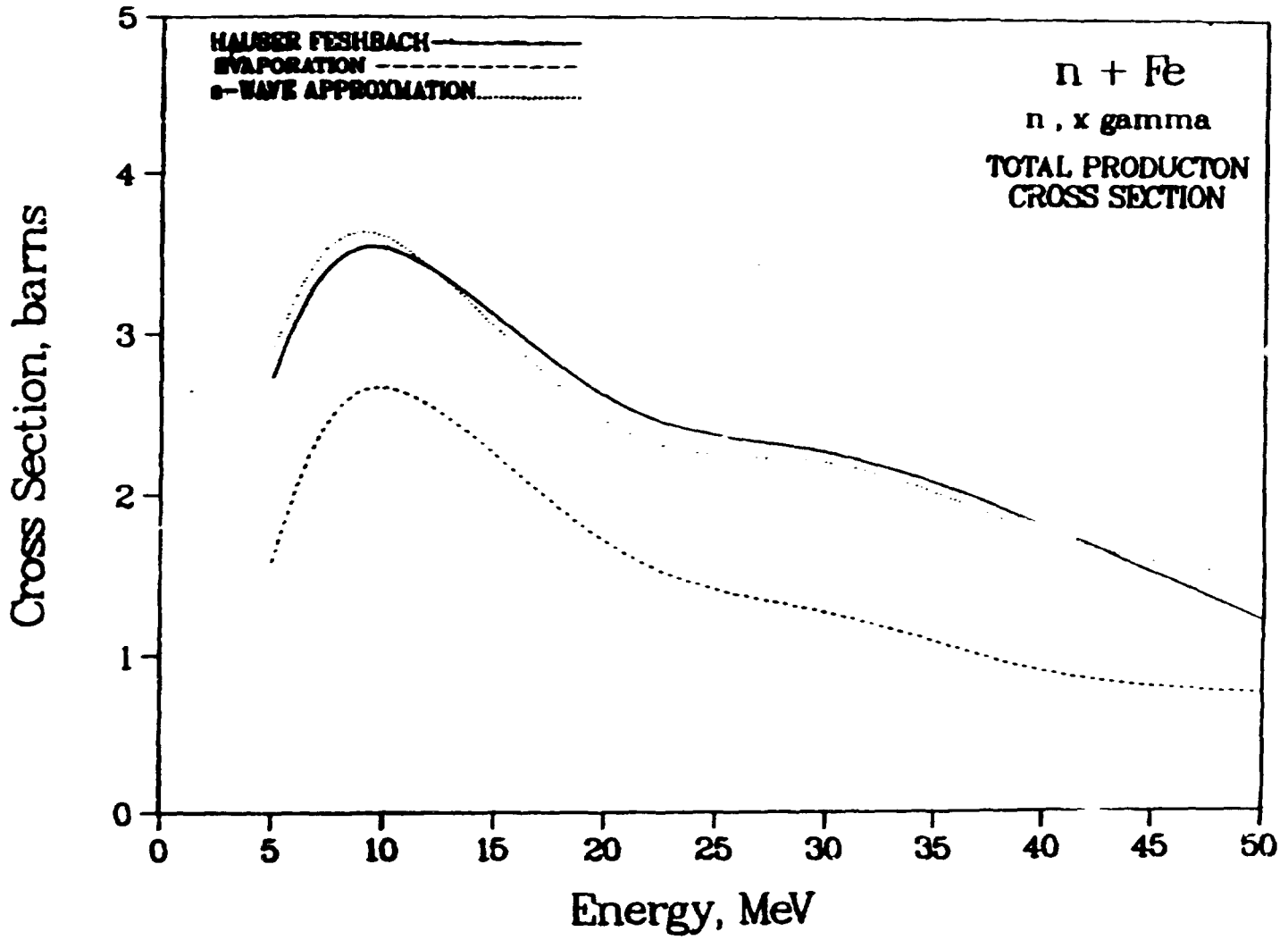


Fig 11



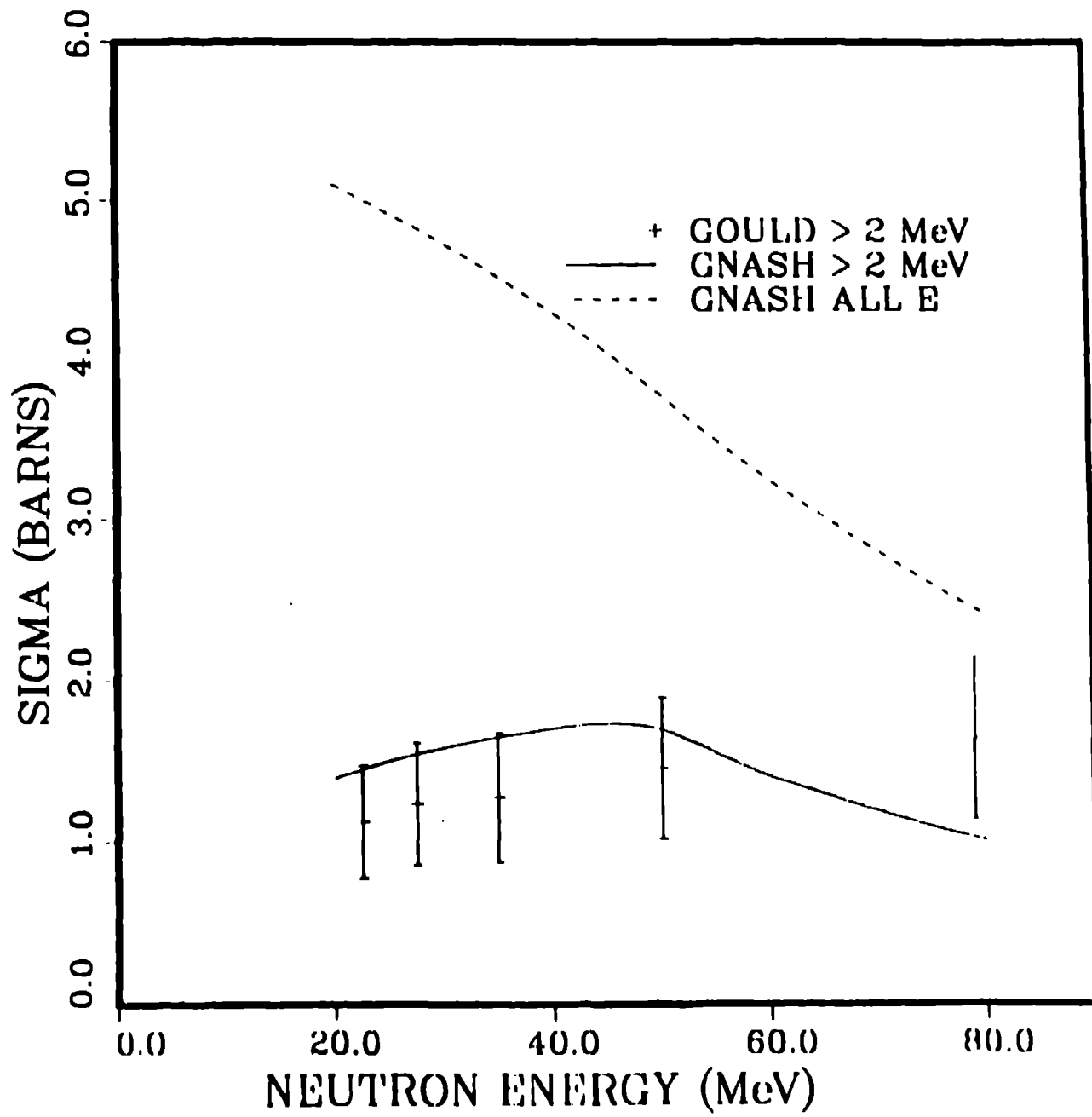


Fig 12

PB208 IGNATYUK,G-C LEVEL DENSITIES

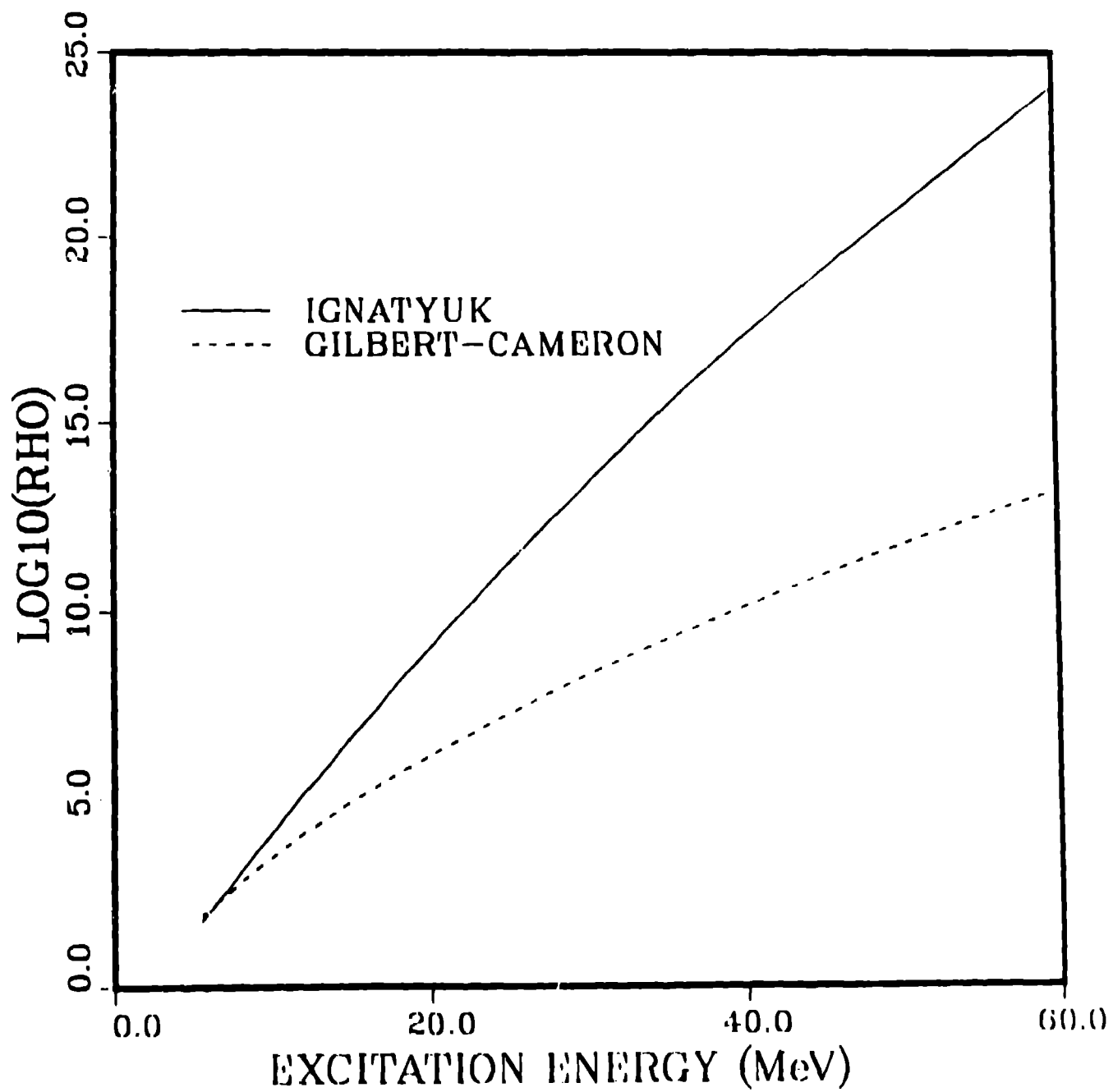
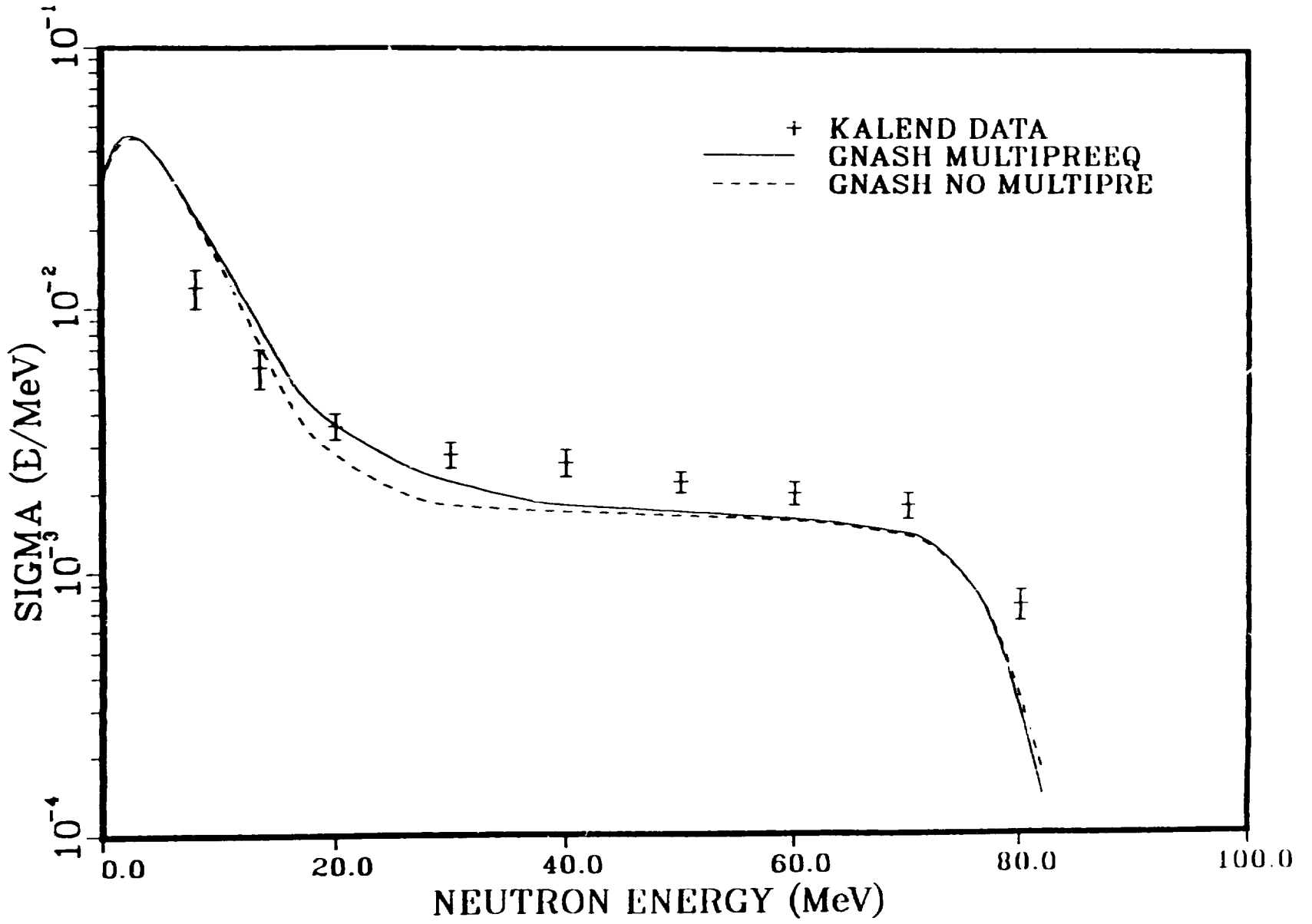


Fig 13

Fig 14





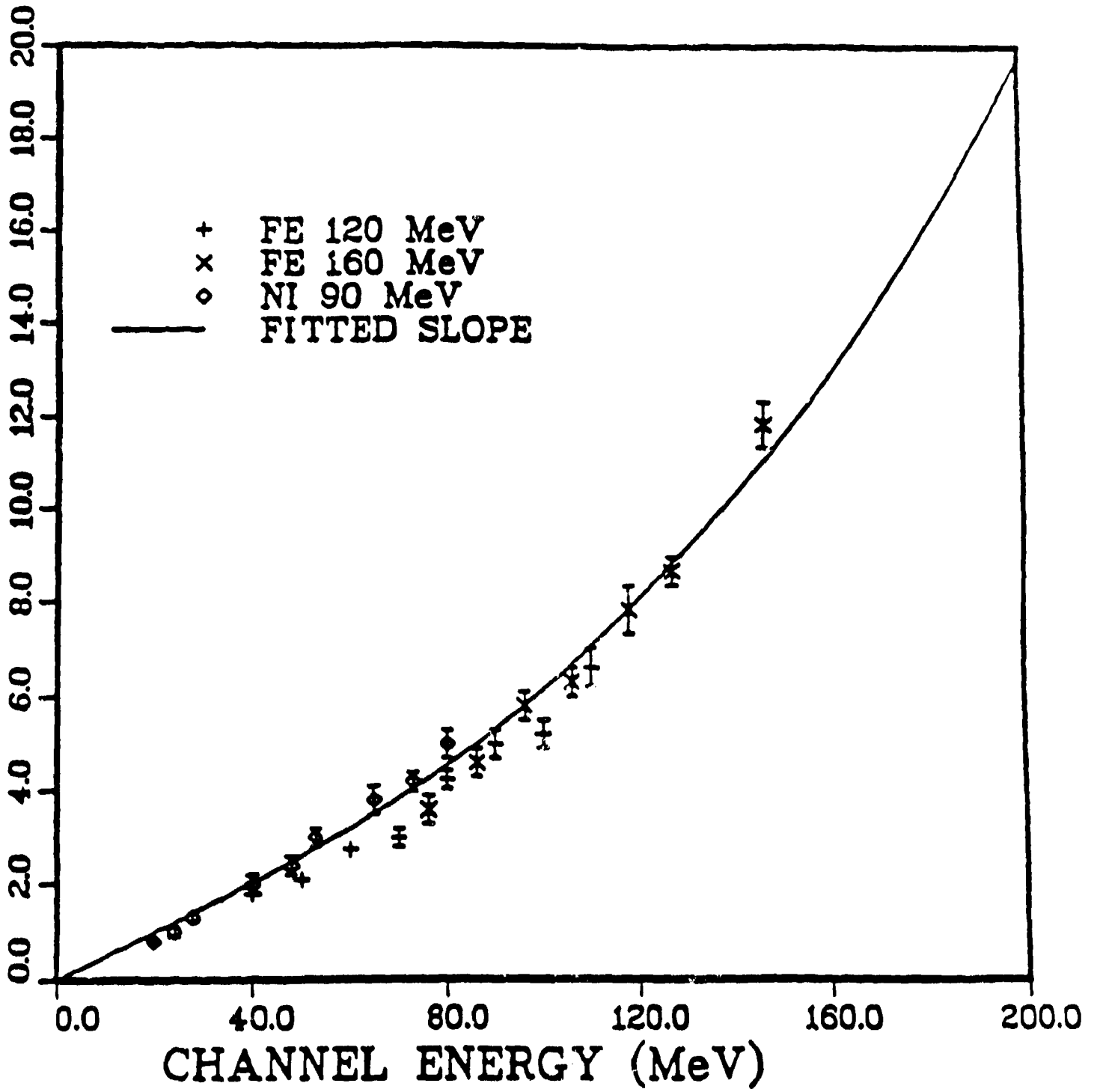


Fig 15

90 MeV  $^{27}\text{Al}(p,n)$  20 MeV exit; 100% MSD

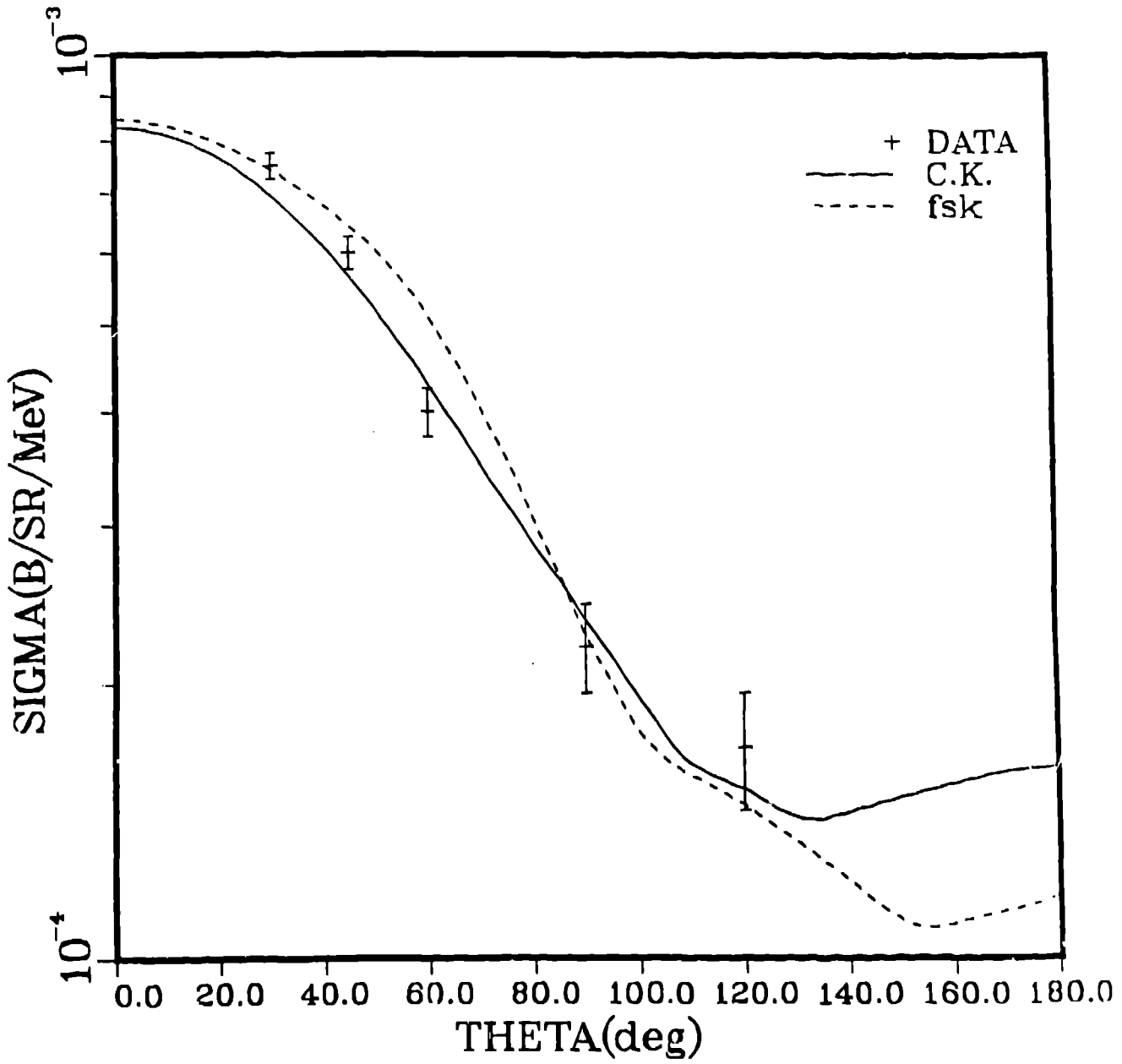


Fig 16

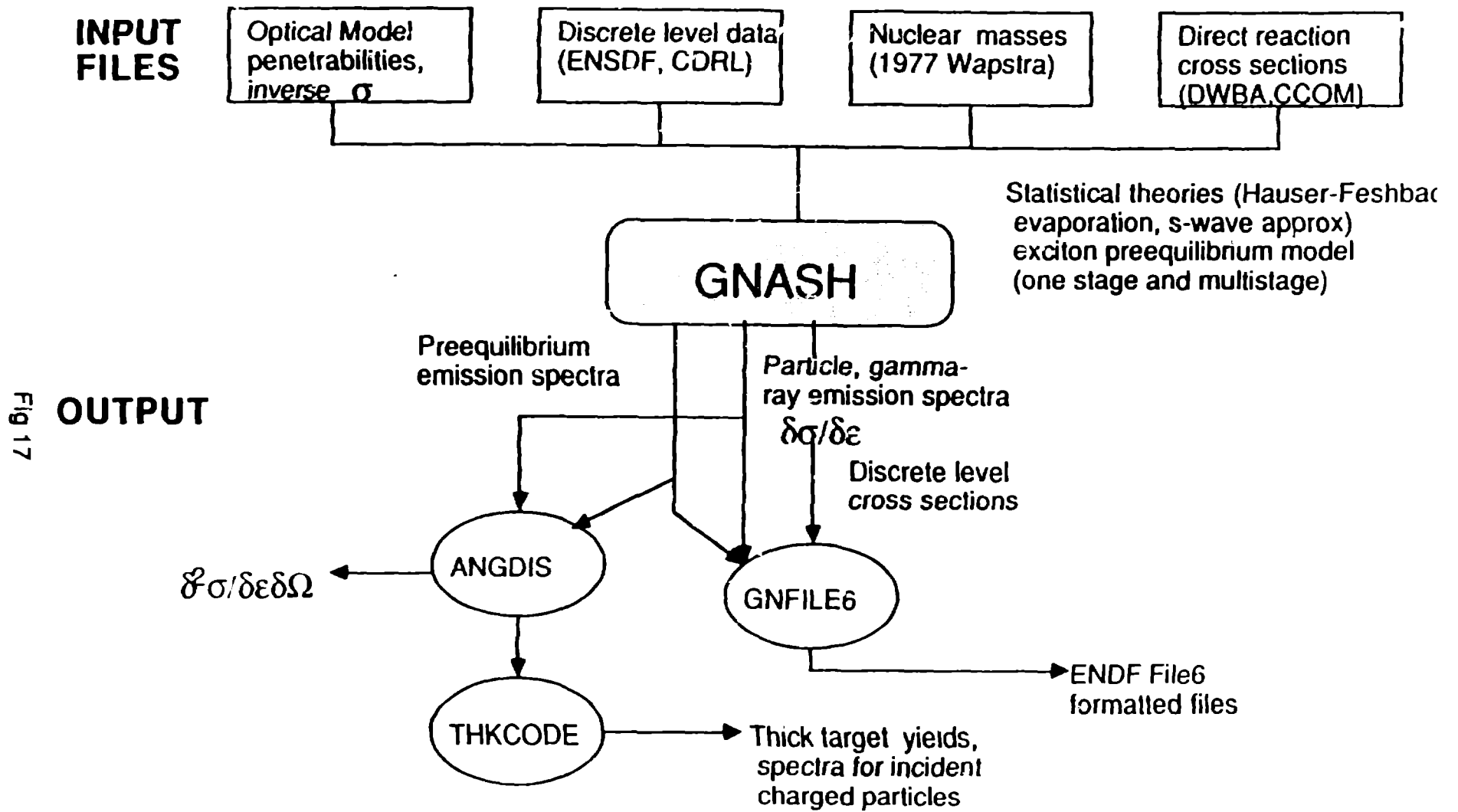


Fig 17